REPUBLIC OF TÜRKİYE

ALTINBAŞ UNIVERSITY

Institute of Graduate Studies

Electrical and Computer Engineering

PERFORMANCE ENHANCEMENT OF LORA COMMUNICATION USING INTERLEAVED CHIRP SPREADING LORA WITH GRAY CODING

Zaid Jameel Radhi KAMOONA

Master's Thesis

Supervisor

Asst. Prof. Dr. Muhammad ILYAS

Istanbul, 2022

PERFORMANCE ENHANCEMENT OF LORA COMMUNICATION USING INTERLEAVED CHIRP SPREADING LORA WITH GRAY CODING

Zaid Jameel Radhi KAMOONA

Electrical and Computer Engineering

Master's Thesis

ALTINBAŞ UNIVERSITY

2022

The thesis titled “PERFORMANCE ENHANCEMENT OF LORA COMMUNICATION USING INTERLEAVED CHIRP SPREADING LORA WITH GRAY CODING” prepared by ZAID KAMOONA and submitted on 09/12/2022 has been **accepted unanimously** for the degree of Master of Science in Electrical and Computer Engineering.

Asst. Prof. Dr. Muhammad ILYAS

Supervisor

Thesis Defense Committee Members:

Asst. Prof. Dr. Muhammad ILYAS	Department of Computer Engineering, Altınbaş University	_____
Asst. Prof. Dr. Abdullahi Abdu IBRAHIM	Department of Computer Engineering, Altınbaş University	_____
Asst. Prof. Dr. Jawad RASHEED	Department of Software Engineering, Nişantaşı University	_____

I hereby declare that this thesis meets all format and submission requirements of a master’s thesis.

Submission date of the thesis to Institute of Graduate Studies: ___/___/___

I hereby declare that all information/data presented in this graduation project has been obtained in full accordance with academic rules and ethical conduct. I also declare all unoriginal materials and conclusions have been cited in the text and all references mentioned in the Reference List have been cited in the text, and vice versa as required by the abovementioned rules and conduct.

Zaid KAMOONA

Signature

DEDICATION

TO MY DARLING FAMILY

I dedicate this thesis to my devoted parents and brothers, who have always instilled in me a belief in Allah, the value of hard effort, and the principle that much may be accomplished with little. And my brilliant, lovely wife, who was standing with me all the time and gave me the courage to complete my work.

TO MY RESPECTED ADVISOR

For me, advisor are a constant source of motivation and inspiration. My advisor remained a guiding light for me on the road that led me to complete my work.

TO MY SPECIAL FRIENDS

To me, my friends are everything. I can confidently state that without their participation, collaboration, and teamwork, I would not be able to easily reach my goal.

ABSTRACT

PERFORMANCE ENHANCEMENT OF LORA COMMUNICATION USING INTERLEAVED CHIRP SPREADING LORA WITH GRAY CODING

KAMOONA, Zaid Jameel Radhi

M.Sc., Electrical and Computer Engineering, Altınbaş University,

Supervisor: Asst. Prof. Dr. Muhammad ILYAS

Date: 12/2022

Pages: (73)

LoRa is One of the LPWAN technologies that refers to long-range communication, which may reach distances of up to three miles in urban areas and ten miles in rural regions. LoRa uses the CSS modulation approach and relies on cyclic shifts of the LoRa base chirp to create a multidimensional signal consisting of nonbinary symbols. The symbol rate and number of bits for each LoRa symbol depend on a spreading factor ranging between 7 and 12. ICS-LoRa Based modulation is a novel multi-dimensional space recently developed using interleaved representations of the standard LoRa chirp signals. ICS-LoRa is a way to improve the data rates of the limited-capacity LoRa networks. Despite having a modulation technique with a greater data rate being one of the most important variables to consider, decreasing the bit error rate as much as possible is an important characteristic of wireless communication features. This thesis evaluated the BER performance of ICS-LoRa in AWGN and Rayleigh fading channels and proposed adding Gray coding to the source data in order to reduce BER. Our results demonstrated that our suggested strategy reduces BER by around 2.2% to 5.6% in AWGN channel and by approximately 4.1% to 15% in Rayleigh fading channel with different spreading factors.

Keywords: BER, Gray codes, ICS-LoRa, LoRa Modulation, LP-WAN

TABLE OF CONTENTS

Page

LIST OF TABLES

Page

LIST OF FIGURES

Page

ABBREVIATIONS

ADR	:	Adaptive Data Rate
AES	:	Advanced Encryption Standard
ASCII	:	American Standard Code for Information Interchange
AWGN	:	Additive White Gaussian Noise
BER	:	Bit Error Rate
CFO	:	Carrier Frequency Offset
CR	:	Code Rate
CRT	:	Chinese Remainder Theorem
CSMA	:	Carrier Sense Multiple Access
CSS	:	Chirp Spread Spectrum
ETSI	:	European Telecommunications Standards Institute
FER	:	Frame Error Rate
HT	:	Hybrid Transmission
ICS-LoRa	:	Interleaved Chirp Spreading LoRa
IoT	:	Internet of Things
LLR	:	Log Likelihood Ratio
LPWAN	:	Low Power Wide Area Networks
NB-IoT	:	Narrow Band Internet of Things
NCC	:	Network-Coded Cooperation
NS3	:	Network simulator 3

PER	:	Packet Error Rate
RSSI	:	Received Signal Strength Indicator
SDR	:	software defined radio
SER	:	Symbol Error Rate
SF	:	Spreading Factor
SIR	:	Signal-to-Interference Ratio
SNR	:	Signal-to-Noise Ratio
SPC	:	Single Parity Check
SPC	:	Single-Parity Check
TSCA	:	Tree-based Spreading factor Clustering Algorithm
WSN	:	Wireless Sensor Network
BPSK	:	Binary phase-shift keying
MAC	:	Medium Access Control

LIST OF SYMBOLS

B	:	Bandwidth
$\omega_0(n)$	:	Base LoRa symbols
R_b	:	Bit rate
N	:	Chip lengths
R_c	:	Chip rate
$\omega_0^*(n)$	:	Complex conjugate of base chirp
$\overline{\omega_m}(n)$	:	Dechirped LoRa symbol
$\mathcal{F}_k(\overline{\omega_m})$	:	DFT output
$\omega_m(n)$	:	Encoded LoRa symbols
H	:	Implicit header mode
t_s	:	Length of one symbol
DE	:	Low data rate
$s(t)$	:	Mathematical model of chirps
f_{max}	:	Maximum frequency
f_{min}	:	Minimum frequency
PL	:	Number of bytes of payload
$T_{\text{ packet}}$	:	Packet duration
$T_{\text{ payload}}$	:	Payload duration
T_{preamble}	:	Preamble duration

$r(n \mid l)$: Received LoRa symbol

$\bar{r}(n \mid l)$: Received LoRa symbol after dechirped

n : Sample time

R_s : Symbol rate

1. INTRODUCTION

1.1 BACKGROUND

In the most recent few years, a revolution has been brought in wireless communication due to the rise in the popularity of low-power wireless new devices. It is anticipated that over fifty billion devices will be connected to the internet through wireless systems. The term "Internet of Things" (IoT) is becoming increasingly common as the number of "things" that are connected to the internet continues to rise. Humans and machines are interconnected today, which has led to IoT technology. Similar to how persons need a communication protocol, devices also require it. IoT will drive digital transformation in the region and allow new improvements to how people connect at home, work, and elsewhere[1]. When moving from a 4th wireless network to a 5th wireless network, there is a time of transition during which there is an increase in the demand for wireless communications which is the future of connecting devices to the internet. LoRa is a technology that falls under the category of Low Power Wide Area Networks (LPWAN), and it uses the spread spectrum method. This technique is well suited for uses that call for data transmission at a modest rate across a considerable distance. Technologies such as LoRa, Sigfox, and Narrow Band Internet of Things (NB-IoT) are examples of LPWANs. (Figure 1.1) illustrates the findings of a comparison research project conducted on LPWAN technology. some of studies demonstrated that LoRa and Sigfox have advantages over other technologies in terms of range, capacity, affordability, and battery life. On the other hand, NB-IoT has several benefits, including lower latency and quality of service[2].

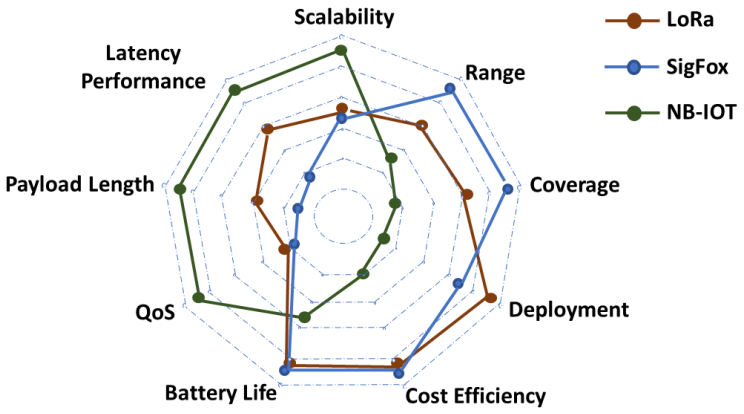

Figure 1.1: Comparison of LPWAN Technologies.

Also, compared to other wireless technologies, such as short-range Wi-Fi, Bluetooth, ZigBee, and long-range cellular communications, LoRa's coverage range is approximately greater than ten kilometers. However, this is dependent on the line of sight. The maximum range and data rate for various wireless technologies are compared in (Figure 1.2).

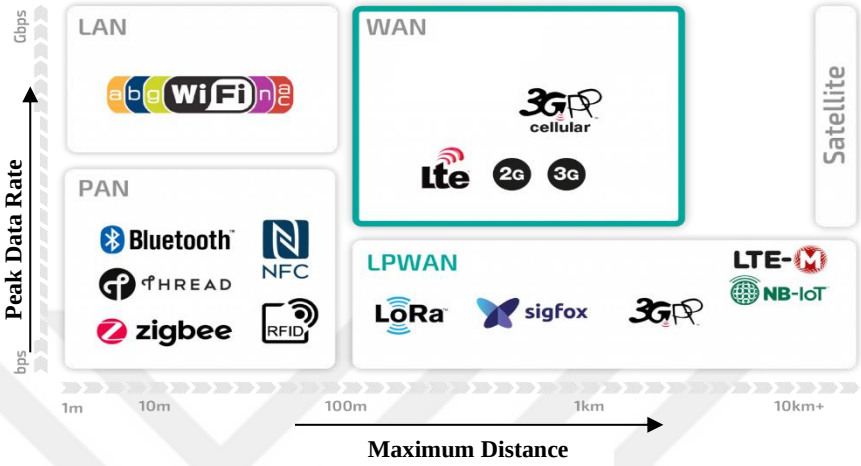

Figure 1.2: Comparison of Wireless Technologies [3].

In 2012, LPWAN did not yet exist, but following its development, LPWAN technology-enabled future communication with extended range, low energy consumption, and inexpensive setup. It was developed primarily for applications needing the transmission of a small number of messages daily across a long range. The predominant technology in this domain is SigFox, LoRaWAN, and NB-IoT[4].

1.2 FEATURES OF LPWAN TECHNOLOGIES

The primary characteristics of LPWAN are Extended Range and Ultra Low power consumption, inexpensive, and scalability[5]. Following is a brief description of each point:

1.2.1 Long Range

Even in challenging indoor environments, LPWAN technology supports providing large area coverage with strong signal transmission at a distance of up to 10 kilometers, and end devices can connect with a base station. To achieve this goal, a variety of features are employed.

1.2.1.1 Sub-GHz Band

The spectrum utilized by LPWAN enables robust connectivity with low power consumption. These frequencies operate well with attenuation and multipath due to obstructions or thick surfaces; these frequencies are not crowded like other frequencies employed in 2.4 GHz wireless technologies, such as Wi-Fi.

1.2.1.2 Modulation

The modulation technique used in LPWAN makes the physical layer transmission bit with high energy so the transmitted signal, even if weak, can be detected well on the receiver side. LoRa technology employs CSS modulation, in which different transmitted channels with quasi-orthogonal transmission result in an increase in capacity and low power consumption.

1.2.2 Operations Using Ultra Low Power

Technology must have extremely low power usage to compete in the market for battery-operated IoT devices. for this, LPWANs mainly use the following techniques:

1.2.2.1 Topology

LPWAN employs a star topology, which is less expensive and simpler to deploy than a mesh architecture. In a star topology, the nodes connect directly with the base station, eliminating the need for a gateway and relays; there is no energy wasted by listening to other nodes. Some LPWANs employ the complicated feature of the mesh design.

1.2.2.2 Duty Cycle

Duty cycle limitations assist LPWAN systems in ensuring that information is only sent or received when required. As a result, power-hungry transceivers frequently turn off in the network's life cycle. Which means it reduces power consumption. popular standards of channel occupation are provided by ETSI and IEEE.

1.2.2.3 Medium Access Control (MAC)

LPWAN utilized ALOHA protocol as a random-access medium access control (MAC) to communicate with receivers without the requirement to detect carriers, hence reducing the cost and complexity of transceivers.

1.2.2.4 Complexity

The base stations handle the complexity of the operations such that the nodes can transmit and receive data on various channels or orthogonally, resulting in minimal energy consumption by the end devices.

1.2.3 Low Cost

In recent years, LPWAN's popularity has expanded due to its inexpensive cost of around $10 and its ability to compete with cellular networks in various applications. In addition, the infrastructure of an LPWAN network is uncomplicated, therefore reducing costs[6].

1.2.4 Scalability

LPWAN has become an essential factor in the development of smart cities by enabling the connection of a large number of distributed devices needed for these services, LoRa can support a range of many kilometers with thousands of low-power units for each base station. theoretically, a small number LoRa gateways is sufficient to offer large-scale connections[7].

1.3 LPWAN TECHNOLOGIES

This section explains several LPWAN technologies, such SigFox, NB-IoT, and LoRaWAN.

1.3.1 Sigfox

Sigfox is one LPWAN technology that provides end-to-end communication solutions in the sub–GHz ISM band. Sigfox employed cognitive SDR in the base station and an IP-based network to communicate with back-end servers. SigFox uses BPSK modulation connects the base station with end devices using the ultra-narrow band (100 Hz). Sigfox utilizes frequency bandwidth properly, leading to low noise levels, reduced energy usage, and high Reception sensitivity with a low-cost price antenna design and a throughput of 100 bps. SigFox utilized a bidirectional approach, uplink up to 140 messages per day with a maximum payload of 12 bytes but downlinking just 4 messages per day with a maximum payload of 8 bytes. Each message is transmitted at multiple times, up to three by default, using a distinct frequency channel; the base station can then receive parallel messages simultaneously.

1.3.2 NB-IoT

NB-IoT can coexist with GSM and LTE on their licensed frequency bands. NB-IoT uses 200 kHz bandwidth, which is equivalent to a single block in GSM and LTE communication, for specific In June 2016 3GPP Release 13 describes Narrowband IoT, and it supported three different procedures, as shown in (Figure 1.4).

a. Stand-alone: Employing the GSM frequencies which is already used.

b. Guard-band: Unused LTE blocks (Guard-band) are utilized in this operation.

c. In-band: using resource blocks inside a carrier for LTE.

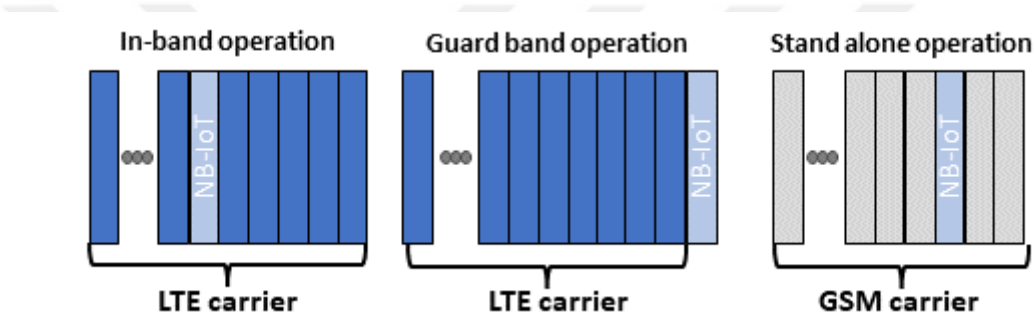

Figure 1.3: Types of Procedure in NB-IoT.

1.3.3 LoRa

Long Range (or LoRa for short) refers to a patented wireless data transmission method. Cycleo of Grenoble, France, invented the technology Semtech purchased in 2012. LoRa's main advantage over other wireless WAN technologies is its excellent range transmission while consuming less power. However, the support for low-bit rate applications places less of a burden on mobility and dependability. Low Power Wide Area Networks (LPWANs), a form of wireless communications vast area network that aims to achieve a +20 dB gain over a conventional cellular system, are supported by this technology[2].This platform is promoted by the LoRa Alliance, which includes companies like IBM, Semtech, and Actility. It proposes a star-of-stars design with specialized gateways serving as transparent bridges between edge nodes and the network core. The data is stored and made available to subscribers. The edge nodes use LoRa (Long Range) modulation to establish one-hop communications with the access points. This is Semtech's unique Chirp Spread Spectrum

(CSS) technique, which utilizes a channel with a bandwidth of either 125 kHz, 250 kHz, or 500 kHz and offers adaptive data rate capabilities via a variable processing gain. This term, commonly known as the Spreading Factor, reflects the ratio between the chip rate and the symbol rate (SF). The LoRaWAN SF ranges from 7 to 12. Using this last characteristic, edge nodes can tune the transmission power and bitrate to the actual network conditions, reducing energy consumption[8].In addition, LoRaWAN classifies edge devices into one of three categories based on the amount of data they require to download: Class A devices have a downloading window that is predetermined and planned immediately after each uplink connection. Class B units have additional downloading windows that are predetermined and scheduled, while Type C units can receive a signal anytime. This means that class A has low power consumption and received signal at any time, and class B works with a coordinated strategy for received signals and has medium power consumption. The last class, C, has a continuous process for receiving signals with extensive power usage[9]. All types explain in (Figure 1.3). The LoRaWAN technology may be used to communicate in unlicensed radio channels designated for industrial, scientific, and medical purposes. In other regions of the world, low-power wide-area networks (LPWAN) are used, and each government establishes its frequency range of LoRa. For instance, the United States uses the frequency range 902-928 MHz (more commonly referred to as the band of 915 MHz); Europe uses the frequency range 867-869 MHz (868 MHz); China uses the frequency range 470-510 MHz (433 MHz); Korea and Japan use the frequency range 920-925 MHz, and India uses the frequency range 865-867 MHz.[10].

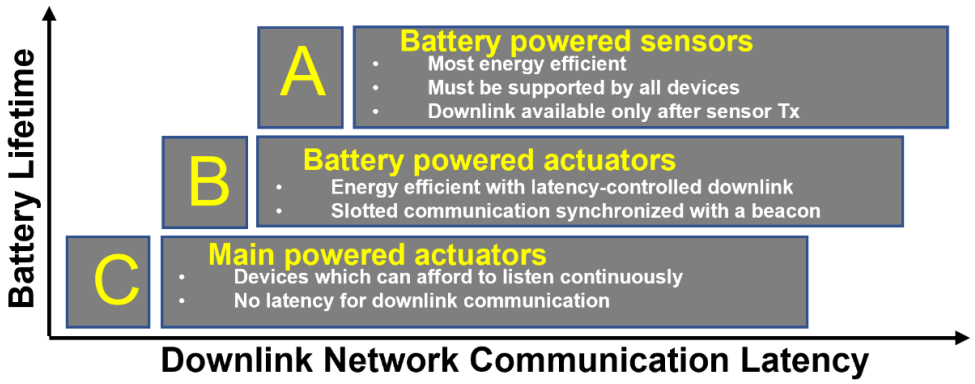

Figure 1.4: Energy vs Communication for All Classes**.**

Sensors enhance the IoT concept by transforming information through wireless communication in normal and harsh environments. Due to these factors, nodes must utilize technologies with long-distance network structures and low energy usage capabilities.

1.4 LORA APPLICATIONS

LoRaWAN is a protocol for wireless Low-Power Wide-Area Networks (LPWAN) that is cost-effective and easily implemented. It supports the transition to Industry by linking remote sensors and equipment, enabling data to be recorded and processed for use in industrial applications. Agriculture, cities, buildings, utilities, and manufacturing are examples of industries taking advantage of this technology. Some Applications of LoRa are maintained below:

1.4.1 LoRa with Oil and Gas

The oil and gas industry are home to some of the world's most complex and mission-critical operations. This is partly due to the remote locations and dangerous environments in which these operations occur, partly due to the engineering and technical expertise required to generate a return on investment, and partly due to the product's essential nature and distribution. Heavy oil accounts for approximately 86% of Chevron's total output from its vast oil field in the San Joaquin Valley in California, operated by the international energy company Chevron, which has its headquarters in the North American continent. The field has a wide variety of assets, most of which are located in different locations, and operators frequently travel to these locations to verify, monitor, and manually document operations. This upstream business has just implemented the LoRaWAN technology, which presents Chevron with an opportunity for a paradigm change. To increase scalability, Chevron deployed gateways using existing radio service providers and remote device management. LoRaWAN sensors were rapidly installed and began reporting data to the cloud. The technology transformed Chevron's manual tank readings into supervisory business control. A significant number of oil and gas companies make use of portable, smaller tanks at client sites. LoRaWAN is a fantastic technology that can monitor the tanks’ levels and track their whereabouts. Sensors produced by Pepperl+Fuchs make it possible for oil companies to

monitor the amount of liquid contained in tanks and get notifications of any issues.Due to the dispersed nature of deployments, asset monitoring is a prominent use case for oil and gas companies in the United States. When working in a major oil field, a firm often has a central office, typically a trailer with its environment regulated. LoRaWAN technology has been installed in these regions by TEKTELIC to maintain track of the trailers, monitor whether or not a trailer is warm, and determine whether or not there are humans in the vicinity. People are not permitted to enter or remain in some dangerous regions for an extended period. Lansitec has implemented personnel and asset monitoring products and solutions with LoRaWAN to assist oil and gas firms in mitigating risk and enhancing management efficacy. This technology may also be used to find all field personnel in an emergency to assist or evacuate[11].

1.4.2 Monitoring of Gas Levels Wirelessly

LoRa devices and wireless RF technology (together referred to as LoRa Technology) are simplifying and lowering the cost of remotely monitoring and managing gas levels using smart metering. Self-reporting gas bottles have the potential to provide intelligence, efficiency, and improved levels of service to the vast consumers that a typical bottled gas distributor is responsible for serving. Conventional storage containers, such as bottles or tanks, can be converted into intelligent devices using long-range, LoRa-enabled wireless sensors. These smart devices can determine their inventory level and relay this data to a cloud-based integrated inventory and scheduling program. To develop its next-generation IoT-based gas bottle level sensing and management application, Butano 24, a division of the Spanish firm Serviglp SL, which processes orders for bottled fuel products on behalf of energy and utility companies, conducted an extensive evaluation of several different wireless technologies. by using LoRA, the resulting system boasts low operating costs, GPS-free geolocation, security, and a high capacity[12].

1.4.3 Fire Detection

Roughly $10 billion in property is lost to flames each year in the United States, and thousands of people are injured or killed. Fires in commercial buildings may quickly spread, so early discovery is crucial for minimizing risk to occupants and property. Firefighters will have a better idea of the scope of a fire and where it is spreading if a system of sensors is in

place to detect flames and smoke. To detect the heat, smoke, gas, or flames related with fires earlier and execute firefighting methods or personnel more quickly, a fire detection system based on sensors and gateways integrated with LoRa Technology based on the LoRaWAN protocol is being implemented[13].

1.4.4 Water Flow Monitoring

Water is becoming scarcer due to the recent rise in extreme weather events, which has led to an increase in coverage of water consumption in the news. Leaks in the architecture of the pipe system are causing a significant volume of water to be wasted. Repairing water leaks and reading meters are two water utilities' most significant operating expenses. Utility companies have the potential to significantly cut their operational costs by putting into place an intelligent water infrastructure. This infrastructure comprises sensors, gateways, automated meter readers embedded with LoRa Technology, and a smart low-pan intelligent area network based on the LoRaWAN protocol[14].LoRa has several further uses, including soil and weather monitoring[15], smart electric metering[16], agriculture[17], gas leak detection[18], and health monitoring[19].

1.5 PROBLEM STATEMENT

Academic and industry researchers have given much attention to LoRa technology, one of the LPWAN technologies, because of its helpful qualities for Internet of Things (IoT) applications. Several studies have been done to evaluate the performance of LoRa and LoRaWAN in a wide range of settings[20]. The LoRa physical layer is designed to have a significant link quality while having a low data rate[21]. For instance, the majority of the currently available research has concentrated on the difficulties associated with increasing capacity, such as [22] other studies have focused on computing the bit error rate with the impact of SNR and SIR, such as [23]. There is still work to be done to fully solve the issue of how to expand LoRa network capacity while simultaneously decreasing the BER.

1.6 RESEARCH CONTRIBUTION

This study decreases the bit error rate (BER) for ICS-LoRa about 2% to 5% in AWGN channel and by 4% to 15% in Rayleigh fading channel with various spreading factors.

1.7 THESIS SCOPE

a. LoRa modulation and demodulation.

b. ICS-LoRa modulation and demodulation.

c. the Gray coding.

d. AWGN and Rayleigh fading channels.

e. Calculate the ICS-LORA BER for different channel types with various SF levels from 7 to 12.

f. Appling Gray coding for the data that be transmitted with ICS-LoRa chirps and then computing the BER for the different types of channels and various SF.

g. Compute the difference in (BER) between ICS-LoRa without Gray coding and ICS-LoRa with Gray coding for different types of channels and various SF.

2. RELATED WORK

Adaptive Data Rate makes it possible to use the capabilities of the LoRa physical layer. ADR is a straightforward technique that modifies the data rate depending on basic principles. Changing the data rate of a LoRaWAN network enables us to quickly expand the network by adding gateways. In addition, the use of ADR can considerably increase the capacity of this sort of network[24]. Although the technology is relatively mature and well-defined, properly allocating wireless resources to accommodate many devices in the same terrestrial region remains difficult. In [25] contributes by suggesting two algorithms of incremental complexity that are demonstrated to perform better than the default Adaptive Rate Strategy ADR. Initially, EXPLoRa-SF demonstrates the advantages of a straightforward approach that does not restrict its usage as ADR but also measures distance and RSSI and chooses Spreading Factors SF according to the total number of devices that are connected to the network. Second, EXPLoRa-AT uses an (ordered water-filling) technique to distribute the spreading factors so that all of the endpoint devices' sent packets to spend an equalize time in the air for each spreading factor group. The primary concept is to integrate SF orthogonality with radio range visibility to increase the number of users who may transmit at once in the network, decrease the number of access collisions, boost the rate at which data is extracted, and therefore raise the throughput. According to simulation results, the proposed algorithms provide vast improvements over the standard ADR strategy. The EXPLoRa-AT algorithm is particularly robust across various operating conditions and provides reliable guarantees of high bit rates even under heavy traffic loads.

The results of some previous research simulations demonstrated that a LoRa network's capacity is increased by combining different communication settings.in [26] simulated a LoRa system with nodes operating at different spreading factors and frequencies. Taking into account both internal and external SF collisions, the author used Poisson processes to represent the packet generating process of each combination and calculated the average packet success probability. A capacity optimization issue was also created for a specified circular deployment region and a required packet delivery success rate. They found a decent approximation to this problem's solution by considering a variety of population sizes and the maximum packet rating of each SF/BW setup. According to the numbers that be gathered, a

sizable percentage of LoRa.Users have achieved perfect settings exceeding 700% as compared to the base scenario where each SF has an equivalent number of nodes.

Every LoRa gateway is capable of supporting six different quasi-orthogonal logical stars network. These networks relate for various LoRa modulation SFs that are accessible. The total capacity of a LoRa gateway is determined by the number of end devices that can be supplied within the connected cell area by all six different spreading factor networks while still achieving certain quality-of-service coverage standards Excellent LoRa signal coverage is mainly attributable to noise limitation and interference restriction factors. In [27] they present a mathematical model developed to analyse the lower as well as upper bounds of the aggregate capacity range of an individual LoRa gateway. This model considers both noise-reduced and interference-restricted coverage issues simultaneously. When coverage likelihood curves are compared to the results of simulations, the suggested coverage measurement model has a high accuracy level. These models' output curves may be used as a development tool for accurately measuring the cell distance and possibly establishing the networks configuration of the single LoRa gateway.

In [28] they attempted to increase their coverage by constructing a multi-hop relay network using direct device-to-device connections. Utilizing this multiple-access dimension, their strategy for increasing the capacity of a multi-hop LoRa network is to offload the data traffic across various subnets. Every subnet originating from a sink node is assigned a unique SF based on network clustering. This makes possible the simultaneous transmission of packets with multiple SFs. They provide a tree-based SF clustering technique TSCA for SF allocations in multi-hop LoRa networks. The TSCA aims to provide connectivity while regulating airtime between subnetworks. According to the study results, there is a significant increase in performance compared to the SF allocation in a single-hop Network system and the tree-based multichannel assignments techniques in WSN.

In[29], they define the capture effect that occurs when two or many LoRa transmissions are happening simultaneously. This study provided an RSSI-based examination of a LoRa non-destructive communication attribute and its effect on the capacity; The characterization demonstrated that when many LoRa transmissions are happening simultaneously, the strongest transmission may be received even if the signal strengths are slightly different. After running simulations of LoRaWAN with various collision models, they found that the

network capacity, particularly in large-scale systems, significantly improved by considering the actual model capabilities. In the end, these findings are applied to evaluating large-scale Low Power Wide Area Networks LPWANs depending on the LoRaWAN protocol, demonstrating that the actual network capacity of LoRaWAN does not correspond to the conventional pure Aloha performance.

SNR and SIR levels are essential factors in LoRa communication, if the target signal meets certain SNR and SIR levels, LoRa signals may keep their coverage area even when facing interference Using a constant spreading factor. In [30][31],The BER performing of the LoRa modulation is estimated numerically as a function of the signal-to-noise ratio and signal-to-interference ratio. The suggested analysis has the benefit of including the combined effect of SNR and SIR on the coverage of LoRa communications subjected to interference with the same spreading factor. in the same LoRa networks, the curves of the BER are useful to determine the coverage zones of SIR as well as SNR.

In [32] Theoretical research and an experimental assessment of the operation (LoRa) technology have been offered. Using a numerical model, they analyzed LoRa's functionality in AWGN Channel in order to better understand the network's communication capability in low signal-to-noise situations. To further investigate the impact of a LoRa CR parameter on system operation, researchers also suggested an analytic BER expression. They have been made an experiment to prove the viability of LoRaWAN across extended distances and to examine the effect of the CR parameter on the system's PER; a controlled experimental setup was designed and built. Measuring about 100 dBm for an SNR 5 dB, transmissions were successful up to 3 km in urban areas and 10 km in open regions. The consistency between the calculated and observed noise levels and the verification of the parameter CR's considerable influence on the system PER demonstrate the practicality of the experimental study for use in the development and implementation of similar LPWAN systems in the future.

In [33] the BER of LoRa signals over Rayleigh and Rice channels have been computed. They have presented accurate numerical formulations of the BER in LoRa systems; however, these expressions are not tractable and include computation precision issues; reason for this is that summing the coefficients of binomials produces tremendous values, which in turn will cause accuracy issues in these formulations.

In [34] they studied the systems after using channel coding; in the first step of this process, they present a matrix model for encrypted communication of LoRa transmissions. In a second step, they build a theoretical model for estimating the bit error for coherent and noncoherent detection of LoRa signals in the AWGN channel, assuming hamming code decoding in the physical layer. The outcomes of their simulation demonstrate that their calculation is accurate. Lastly, the findings of their research confirmed its efficacy in multipath channels and revealed the important LLR calculation technique for soft coding.

In [35] They analyze the error rate performance of LoRa. They strongly estimate BER in the AWGN channel for uncording LoRa modulation. Their work depends on the intelligent adjustment of a union bound on the BER probability. And they discover that their method of calculating BER gives good results with orthogonal and quasi-orthogonal LoRa and is easier to compute than previous methods for orthogonal signals. Additionally, they use simulation to examine the BER for soft decoding LoRa in channels with multipath and offer a technique to compute BER for LoRa systems with Hamming-codded and hard decoded. This method is excellent for low-power devices and delivers close to a 1 dB SNR gain over hard decoding.

AES techniques are sophisticated and need additional energy when utilized with LoRa communication systems with restricted hardware resources. In [36] They suggested a low-cost novel algorithm for physical layer decoding based on LoRa modulation parameters. The technique combines a method for private key retrieval based on the RSSI with a method for sharing classified information based on CRT theory. And demonstrated that their method could protect LoRa communications more effectively than LoRa without encryption, with no loss in BER across varying SNR. This encryption method provides a novel approach to meeting the challenge of securing increasingly widespread IoT deployments.

In [37] They proposed a new method to cancel interference at the receiver and decode the signal from two collision users transmitting in the same SF channel. Using both soft decoding and soft demodulation, they retrieve the interfering signals for each user and can effectively demodulate interference signals on the receiving side with a 1.5 dB power difference.

In [38], they studied BER for LoRa networks by introducing a novel approach that works with the LoRa physical layer by employing the turbo code; their findings indicate that they

enhance data transmission performance in networks and improve spectral efficiency and reduce energy consumption.

In [39], they proposed researching the performance of LoRa communication when it operates with NCC, which means that end devices can send a large number of frames in linear combinations operated over a nonbinary finite field and consider the connectivity and probabilities while estimating the outage probability of an End Device in addition to the energy-consuming to compute Energy efficiency. Their results showed that NCC-LoRa improves energy consumption and outage probability.

In [40], They explained why LoRa is preferable to other IoT LPWAN devices in the industry. However, there is no exact technique for assessing the scalability and reliability of the LORAWAN protocol currently available. Message replication is a technique used to increase the reliability of LORAWAN connections by transmitting data in segments at various times. In this work, they developed a novel hybrid approach for message coding that interleaves basic repetition with coded form. In addition, they provide information on the relationship between the number of endpoints in a network and the probability of an outage, taking communication and collisions into account. The findings of this study demonstrated that hybrid transmission improves LoRa communication by making it more flexible and configurable with many parameters, hence increasing its reliability. Finally, they compared the power consumption of hyped transmission to both main replication transmission and codded transmission. Both have equivalent outcomes.

In [22] the researcher explains how LoRa demonstrated its effectiveness over other IoT devices. LoRa utilized Chirp spread spectrum modulation with six quasi-orthogonal distinct spreading factors; when the spreading factor (SF was raised, the distance of the sent signal was extended, but the data rate was reduced. LoRa can transmit with six spreading factors simultaneously, whereas LoRa uses the ALOHA technique for transmissions inside the same spreading factor network. Because of data collisions, this approach had a limited capacity. To increase the capacity limit of LoRa communications, they provided SPC codes with soft encoding decisions in this work. In the beginning, the LLR was driven by decision-making. The findings demonstrated that when SPC is applied, there is a power gain of around 1.2 dB; this gain occurs when activating and disabling SPC in the same network with the same

spreading factor since the data transmission time has been shortened. The improvement with capacity scaling improved by approximately 65% compared to LoRa without SPC.

In [41] they evaluate coding FER of LoRa in both AWGN and interference channels with CFO. Initially, they used a model to compute BER, which they obtained from other studies, and then they presented a new model for computing BER for LoRa frame error rate in AWGN channel with less complexity; they found that the results at 0.2 dB in Monte Carlo simulation decreased by approximately 10^{-5}. Moreover, they developed an alternative approach for calculating FER in the interference channel. The results of this approximation expression demonstrated that LoRa could reduce the effect of CFO by using Gray, interleaving, and whitening. Lastly, they present a second model that provides an approximation expression for LoRa FER in interference channels, but it has 0.5dB more than the first simulation method.

In [42], the researchers explain how the modulation technique transmits data, how the ALOHA approach limits capacity, and how detecting the channel affects collision problems. In conclusion, they describe how serial interference cancellation could improve communication performance and determine when a random location for simultaneous transmission could result in effective decoding at the receiver.

In [43], they attempted to use a custom-designed board on the transmitting side to communicate sensor data. Using ASCII and Huffman codes, two approaches for transmitting data have been evaluated. The results of the two approaches have been computed in order to compare them.in this practical test, they employed varied spaces up to 1 km distances and collected up to 250 data sets from both transmission techniques. The results of this test indicate that data compressed with Huffman is approximately 40% smaller than data compressed using ASCII. This indicates that this approach uses Huffman codes to improve transmissions from multiple devices in parallel. When the transmission distance increases, the error rate increases, however the Huffman code is able to reduce the error rate from 24.7% to 20.6%.

In [44], they used the NS3 simulation program to simulate a new model for the LoRa network with accurate performance and then compared the results gathered from this model with other practical results found in other studies; this model could show the correct packet drop

rate that results from data collisions; in this model, they attempt to improve LoRa network performance and power consumption. They calculated CSMA in their simulation and examined the effect of the LoRa communication; they found that the outcomes have reduced the collision ratio with an increase in power consumption, but they noticed that when they used CSMA with a large number of end devices, the power consumption was decreased; they also discovered that CSMA and CSMA -10 increase the capacity and throughput due to ETSI.

In [45], they evaluated the communication performance of LoRa networks in the AWGN channel and interference channel, extended the basic method of interference to a more realistic method in which the interfering user's chip and phase cannot be aligned with the signals, and developed a new model for calculating error rate. They find that the primary method does not produce high accuracy. They demonstrate that interference signals have two symmetrical, so they develop a new model to compute SER and FER with low complexity. Finally, the used simulation to corroborate with the theoretical model to produce more accurate results.

In [46], Reverse engineering has been used in this research; They proposed a novel closed-form model for all the stages that occur in LoRa modulation, coding, and interleaving inside the physical layer for both the transmitter and the receiver. These equations allow for the simulation-based investigation of LoRa performance across known channels. This model enables researchers to evaluate the efficiency of LoRa networks with any channel. Using simulation, also they determined that when quadrature modulation was combined with chirp spread spectrum, modulated signals were preferable to coherent and noncoherent methods at the receiver side. That chirp spread spectrum performs well when transmitted over time and frequency selective channels. Finally, they discovered that the performance was enhanced when soft decoding, whitening, and interleaving were combined with the chirp spread spectrum compared to the chirp spread spectrum alone. Nonetheless, it suggests an increased reception complexity, which might be significant for base stations.

Recently Due to the increasing number of nodes in the same networks, WSNs used for IoT require a positioning algorithm with low complexity. The fundamental localization RSSI model is an attractive model for LPWANs such as LoRa; nevertheless, when the RSSI model is used in network systems, it causes a few localization mistakes. In [47], they introduced a

new, low-complexity method to enhance the localization approach based on a winner-based model. They defined the range as an exponential function of the gathered RSSI. This model reduces distance model errors, provides a more accurate range and location, and investigates the variety of information received at the physical layer with different data rates and bandwidths. These findings are more successful than the standard approach used for RSSI localization.

In [48], they utilized ICS-LoRa to synchronize with basic LoRa to reduce collisions when basic LoRa employs the ALOHA model and limits data transmission. The orthogonal shift between the spreading factors in LoRa signals enables it to send six transmissions in parallel without interference, and ISC-LoRa might function as a new multidimensional and transmit in parallel with other six spreading factors. The simultaneous transmission of LoRa and ISC-LoRa results in a strong cross-correlation of the transmitted signals at the receiver. In addition, they proposed a new method for determining BER for this system and compared their BER result with the simulation result; the results are very approximative. The mathematical model is used to determine signal-to-interference and signal-to-noise ratio coverage zones in order to calculate the parallel transmission capacity across standard LoRa and ICS-LoRa. The results indicate a high level of accuracy between the driven analytical model and the simulation model, with just a 3.39% error. they Utilizing software defined radio (SDR) to implement mathematical technique and simulation practically, this simultaneous transmission of ICS-LoRa and standard LoRa with six spreading factors increases capacity by 42%.

3. METHODOLOGY

This chapter explains the LoRa and ICS-LoRa modulation and demodulation schemes, as well as the chirp spread spectrum and the Gray mapping code. Finally, the system model is described by adding Gray code to ICS-LoRa.

3.1 LORA PHYSICAL LAYER

LoRa is a unique spread spectrum modulated method derived from Chirp Spread Spectrum modulation (CSS) that trades data rate with sensitivity inside a defined channel bandwidth. It utilizes orthogonal spreading factors to provide a changeable data rate, allowing the system designer to exchange data rate for distance or power consumption in order to improve network performance in a given bandwidth[49].

3.1.1 Chirp Spread Spectrum

LoRa physical layer uses the Chirp spread spectrum as a modulation technique. This process allowed LoRa to transmit data over a wide area using the 868 MHz frequency spectrum. LoRaWAN implements variable bandwidth (125,250,500) KHz based on distance, noise, and bandwidth; SF has chosen to transmit the signal without affecting the noise.

3.1.1.1 CSS symbols

Each symbol in chirp spread spectrum modulation is influenced by four essential factors: SF, minimum frequency, maximum frequency, and inputs bits. to produce CSS symbols, it needs a start frequency which is between f_{max} and f_{min}, provides the $log_2(SF)$ bit data input. After that, the symbol's length could be determined. The value of each symbol period, t_s is given in Eq. (**3.1**)

$$t_s = \frac{SF}{B} = \frac{SF}{f_{max} - f_{min}} \tag{3.1}$$

B represents the bandwidth, which is equal to the difference across f_{min} and f_{max}. Eq. (3.2) used to determine a bit rate R_b**:**

$$R_b(SF) = \frac{\log_2(SF)}{t_s} \tag{3.2}$$

Whenever the symbol duration is specified, the signal chirps continuously from frequency f_0 to frequency f_{max} and from frequency f_{min} to frequency f_0. Eq. (**3.3**) provides the mathematical model of chirps. (Figure 3.1) illustrates two chirps, one with a spreading factor and the other with a half spreading factor.

$$s(t) = e^{i2\pi f(t)t} \tag{3.3}$$

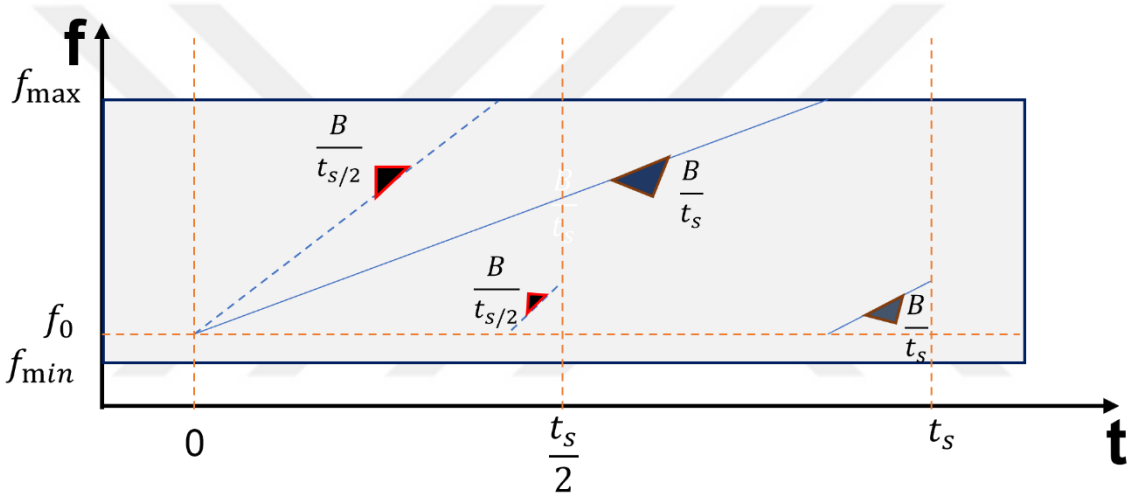

Figure 3.1: Frequency vs Time for Two Chirps.

3.1.1.2 Decoded Symbols

CSS symbols are quasi-orthogonal. Therefore, the decoder uses the correlation technique to detect the signal; transmitted symbols correlate with the CCS base symbol. The decoder then selected the specific chirp with the highest correlation [50].

(Figure 3.2) Represent an example of up chirp, which occurs when the signal begins at a low frequency and increases in frequency, and down chirp, which occurs when the signal begins at a high frequency and decreases in frequency. and it was plotted using MATLAB.

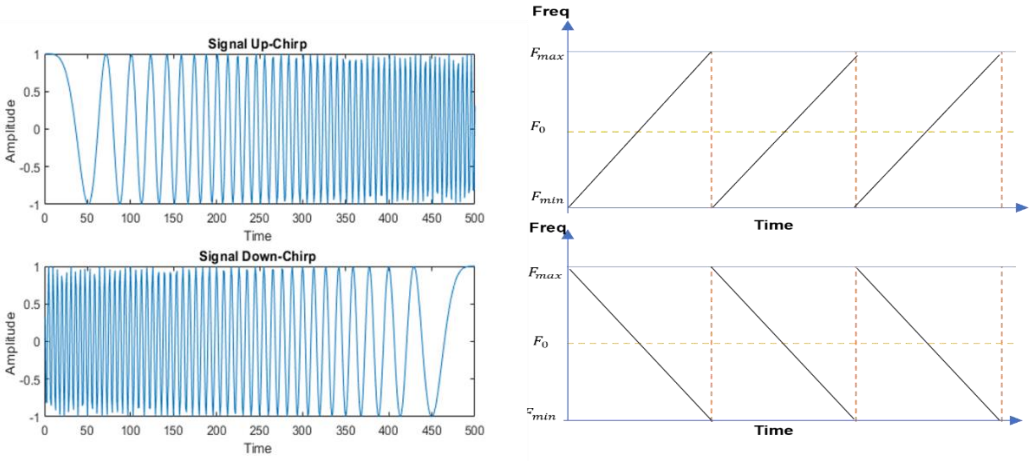

Figure 3.2: Frequency vs Amplitude for CSS Plotted by MATLAB.

3.1.2 LoRa Chips, Symbols, Chirps, and Spreading Factor

The chip is an encoded pulse that sweeps from low to high frequency in bandwidth. Many chips are used to encode every bit of data. The sum of neighboring chips produces a symbol. The desired LoRa modulation data bit rate is given in Eq. (**3.4**)

$$R_b = SF * \frac{1}{\left[\frac{2^{sf}}{B}\right]} \tag{3.4}$$

Each chip corresponds to a one bandwidth pulse Eq. (**3.5**)

$$R_c = \frac{1}{\mathrm{B}} \tag{3.5}$$

Where SF = [7, 8, 9, 10, 11, 12]. this means 2^{SF} sets of symbols can be sent through the BW. Consequently, the symbol rate corresponds to the Bandwidth expressed in Eq. (**3.6**)

$$R_s = \frac{B}{2^{SF}} \tag{3.6}$$

LoRa was developed for symbol groups of chip lengths N ∈ {128, 256,512, 1024, 2048, 4096}. Eq. (**3.7**) illustrates SF in terms of N[51][49].

$$SF = log_2\,(N) \tag{3.7}$$

The LoRa PHY employs six spreading factors ranging between SF 7 to SF 12 and three bandwidths (125 kHz, 250 kHz, and 500 kHz). Due to the CSS approach, data with varied data rates could be viewed as series of orthogonal virtual channels. As a consequence, the total capacity has been raised. (Figure 3.3) represent a comparison of LoRa chirps in six spreading factors[52].

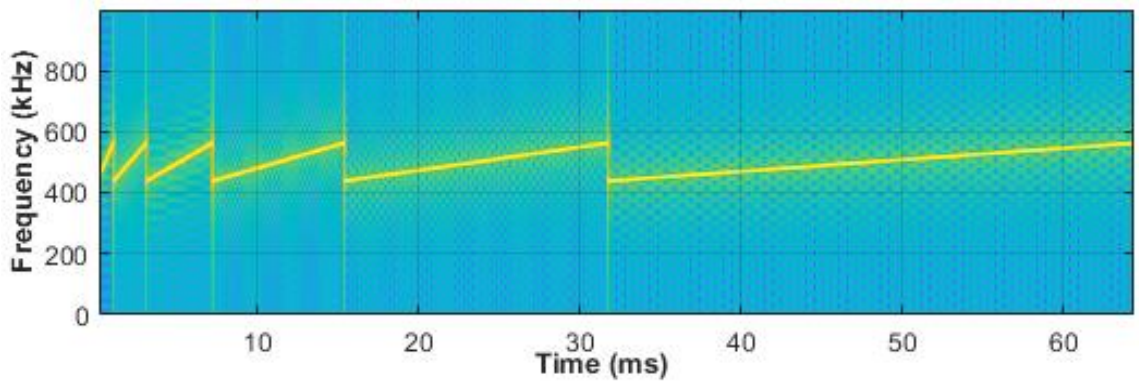

Figure 3.3: Comparison of LoRa Spreading Factors: SF 7 to SF 12 Plotted by MATLAB.

3.1.3 LoRa Packet Architecture

The LoRa modem utilizes either explicit or implicit packet formats. The explicit packet provides a small header that defines the bytes, the code rate, and the status of a CRC. (Figure 3.4) below illustrates a packet format.

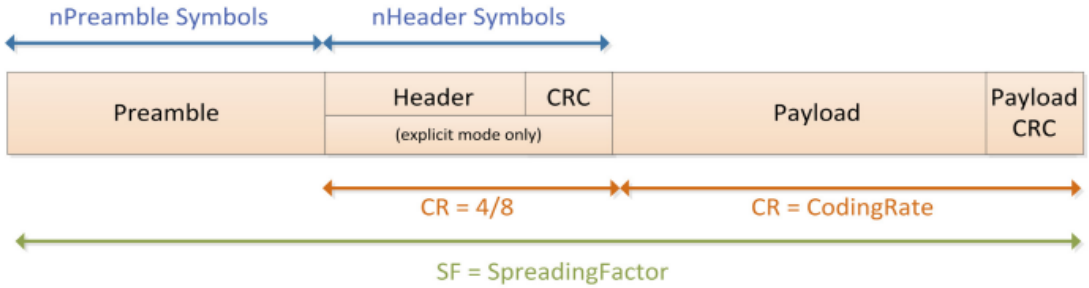

Figure 3.4: LoRa Packet Architecture [53].

Each LoRa packet consists of three components: preamble. Optional header. The payload of data.

3.1.3.1 Preamble

The preamble is utilized to align the receiving device with the receiving data flow. The packet is originally configured with 12 symbols, which can be changed. The preamble length should be set to the same length as the transmitter's preamble length. The receiver detects the preamble length, which repeats in a constant period. If the preamble is unknown or variable, the receiver will set it.

3.1.3.2 Header

There are two types of headers: explicit and implicit, in Explicit Mode (default mode), the length of the payload, the CRC code rate, and the header CRC are transmitted over the header to the receiving device. While in Implicit Mode the header of the packet is deleted. So, payload duration, CR, and status of the payload CRC are manually set on the transmitter and receiver sides of the radio connection. Implicit header mode helps to reduce the time of transmitting.

3.1.3.3 Payload

This packet Is the field that contains data encoded with an error rate that will be specified in the header when the explicit mode is used, or that will be set manually when the implicit mode is used[53].

3.1.3.4 Forward Error Correction

Forward Error Correcting (FEC) is the technique of adding error correction bits into transmitted data. These extra bits assist in the recovery of data that has been distorted by interference. The addition of extra error-correcting bits leads to data correction. However, increasing the number of error-correction bits reduces battery life.

3.1.3.5 Coding Rate

The coding rate is the proportion of transferred bits that carry information. LoRa allowed coding rate values: CR = 4/5, 4/6, 4/7 or 4/8. (Figure 3.5) is an illustration of the ratio between transmitted bits and coding rate when SF = 8[51].

Figure 3.5: Proportion between Transmitted Bits and Coding Rate when SF = 8.

3.1.4 Packet Time on Air

ToA is a measuring unit for the duration of time that LoRa packets were transmitted. as shown in (Figure 3.6).

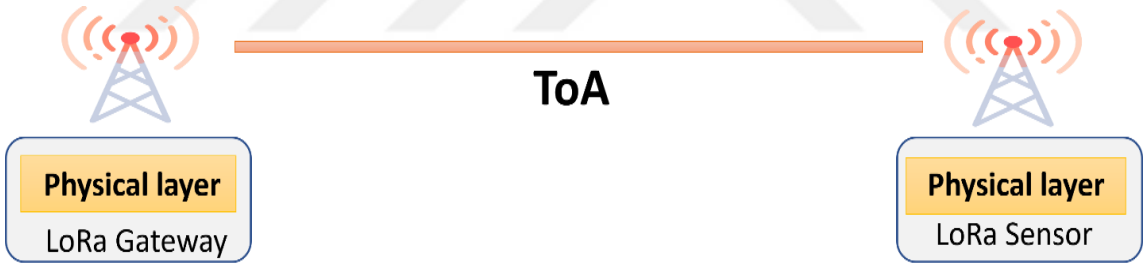

Figure 3.6: LoRa packet Time on Air.

Each LoRa packet is composed of both a preamble and payload symbols. Therefore, T_{packet} equals the total of preamble T_{preamble} and payload T_{payload} lengths. The duration of a symbol T_s can be expressed in Eq. (**3.8**)

$$T_s = 1/R_s \tag{3.8}$$

In [54] , T_{preamble} is presented in Eq. (**3.9**)

$$T_{\text{preamble}} = \left(n_{\text{preanble}} + 4.25\right) * T_s \tag{3.9}$$

From[54] (n_{preanble}) is configurable by programming, and it has two sorts of settings: RegPreambleMsb and RegPreambleLsb, the purpose of which is to save the preamble duration.

Eq. (3.10) is used to obtain T_{payload}:

$$T_{\text{payload}} = n_{\text{payload}} * T_s \tag{3.10}$$

n_{payload} can be computed with the following formula Eq. **(3.11)**:

$$n_{\text{payload}} = 8 + \max\left(\text{ceil}\left(\frac{8PL - 4SF + 28 + 16 - 20H}{4(SF - 2DE)}\right)(CR + 4),0\right) \tag{3.11}$$

where PL represents the payload size in bytes and SF is the spreading factor. H indicates the state of the header, which is 0 for implicit mode and 1 for explicit mode. DE = 1 if low data rate improvement is enabled, and DE = 0 if it is disabled. CR Is the rate of coding between 1 and 4.

Accordingly, the total packet Time on Air T_{packet} is shown in Eq (**3.12**):

$$T_{\text{packet}} = T_{\text{preamble}} + T_{\text{payload}} \tag{3.12}$$

(Figure 3.7) shows the total time on air for a packet containing a preample and payload.

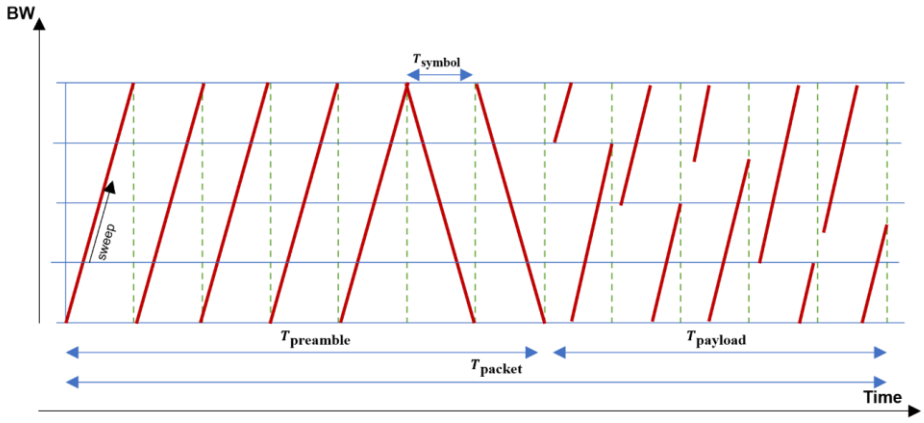

Figure 3.7: Total Packet Length.

3.1.5 Adaptive Data Rate

Adaptive data rate (ADR) is a fundamental aspect of IoT architecture and an exciting feature. It enables high network throughput and enhances network scalability. Using ADR, the LoRa network can optimize the power consumption, distance, and capacity of end devices. This functionality is extremely useful for projects involving a large number of end devices LoRa system gives end devices the ability to decide on the suitable data rate and transmission power [9]. Nodes located near the gateway transmit data at a high rate. For example, SF is 7. Therefore, they have less time in the air and use the low link budget they require. For nodes with large distances, the data rate and linked budget are increased, for example, SF=12. In addition, the length of airtime necessary for a device to transmit its payload is enhanced, drastically reducing power consumption. (Figure 3.8) shows the output of a simple situation in which they employ a free space path loss environment to calculate the attenuation between the gateway and the end device[55].

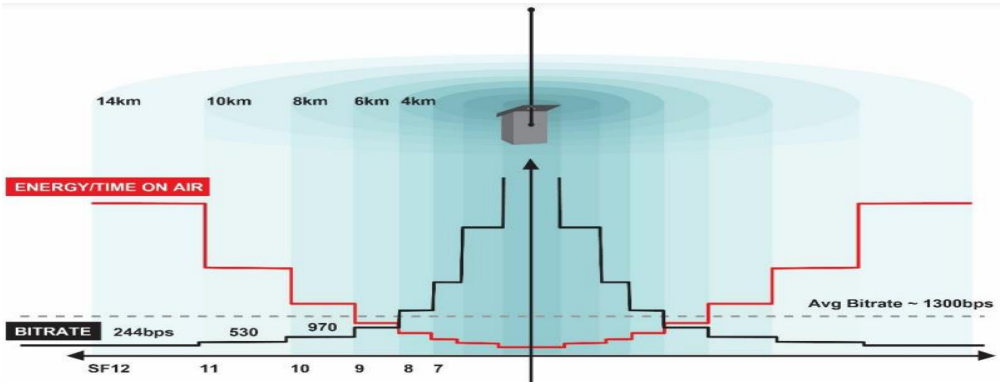

Figure 3.8: LoRa Packet Bit Rate vs. Energy Downlink in Free Path Loss Situation [55].

3.2 LORA MODULATION

The chirps are cyclically shifted, and the frequency jumps define how the data is encoded onto the chirps. It is known that each symbol contains one or more data bits. For example, symbol=1011111, which is equal to 95 in decimal, and the number of raw bits that the symbol can encode is seven which means SF=7, and each symbol has 2^{SF} values or chips. (Figure 3.9) shows a symbol value contained inside 128 chips.

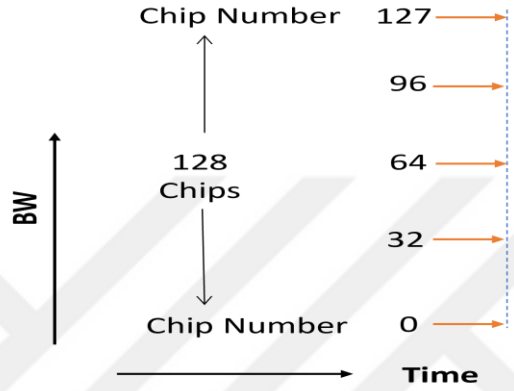

Figure 3.9: An Illustration of a Symbol has 128 Chips.

As an illustration of modulated information, consider the binary value 1100000, which is equivalent to 96 in decimal. The row bit length for symbol encoding is seven, thus the spreading factor is also seven, and the chirp was divided into 2 ^{sf} chips. as seen in (Figure 3.10) The chirp begins at value 96 and ends at 128 before shifting cyclically from 0 to 95 [51].

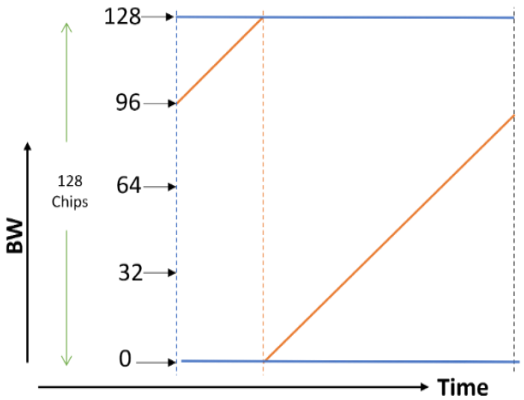

Figure 3.10: Cyclically Shifted Modulated Information (1100000).

3.2.1 Normal LoRa Modulation and Demodulation

In the standard LoRa modulation, LoRa symbols might be viewed in terms of discrete shifting cyclically in time of some base Chirp Spread Spectrum discrete-time signal $\omega_0(n)$ that is presented in Eq. (**3.13**) [56]:

$$\omega_0(n) = \sqrt{\frac{1}{2^{SF}}} \exp\left[j2\pi \cdot \frac{n^2}{2^{\mathrm{SF}+1}}\right] \tag{3.13}$$

Where $n = 0,1,2,\dots,2^{SF} - 1$ represents the sample time position, and $SF \in \{7,8,9,10,11,12\}$ is the spreading factor that defines the symbol length T_S which is composed of 2^{SF} samples.

According to [56], the standard LoRa modulation might be produced by deploying 2^{SF} cycling time-shifts of the basis chirp signal $\omega_0(n)$ to encode 2^{SF} different LoRa symbols $\Omega_m = m, m \in M = \{0,1,2,\dots,2^f - 1\}$. Consequently, let us describe $\omega_m(n), m \in M$ as a LoRa chirp signal formed from the m^{th} cyclic time shift of $\omega_0(n)$ such that $\omega_m(n)$is defined in Eq. (**3.14**).

$$\omega_m(n) = \sqrt{\frac{1}{2^{SF}}} \exp\left[j2\pi \cdot \frac{((m+n) mod 2^{SF})^2}{2^{SF+1}}\right] \tag{3.14}$$

LoRa demodulation in a standard LoRa receiver consists of two basic steps: Dechirping, which means multiplying the transmitted LoRa signal by the complex conjugate of the signal's basis chirp, $\omega_0(n)$, second step is DFT [57] as Eq (**3.15**).

$$\bar{r}(n \mid l) = r(n \mid l) \times \omega_0^*(n) \tag{3.15}$$

where $r(n \mid l)$ represents the LoRa signal received given $\Omega_l = l$ represents the sent symbol, while $\bar{r}(n \mid l)$ represents the received signal after dechirping and $\omega_0^*(n)$ is the complex conjugate of a basic chirp signal $\omega_0(n)$. from[56] each chirp of dechirped LoRa $\overline{\omega_m}(n)$ described in Eq. (**3.16**):

$$\overline{\omega_m}(n) = \frac{1}{2^{SF}} \cdot \exp\left(j2\pi \cdot m \cdot \frac{n}{2^{SF}}\right) \cdot \exp\left(j\theta_m\right) \tag{3.16}$$

Where θ_m is given in Eq. (**3.17**)

$$\theta_m = 2\pi \cdot \frac{m^2}{2^{SF+1}} \tag{3.17}$$

After dechirping of the receiving signal, the DFT applied to the dechirped signal. k^{th}represent the output after DFT $\mathcal{F}_k(\overline{\omega_m})$ applied to $\overline{\omega_m}(n)$ which is computed in [56] as Eq. (**3.18**).

$$\mathcal{F}_k(\overline{\omega_m}) = \frac{1}{2^{SF}} \cdot \exp\left(j\theta_m\right) \cdot \sum_{n=0}^{2^{SF}-1} \exp\left(j2\pi \cdot (m-k) \cdot \frac{n}{2^{SF}}\right) \tag{3.18}$$

Because $|\exp(j\theta_m)|$ equals 1 and $(m-k), \forall m, k$ represents an integer, the magnitude of $\mathcal{F}_k(\overline{\omega_m})$ is Eq (**3.19**).

$$|\mathcal{F}_k(\overline{\omega_m})| = \begin{cases} 1 & k = m \\ 0 & k \neq m \end{cases} \tag{3.19}$$

Therefore, the receiver selects the DFT result value with the greatest magnitude to detect the sent LoRa symbol. (Figure 3.11) illustrate the operation of dechirping by multiplying the chirp signal by the complex conjugate of the base chirp signal.

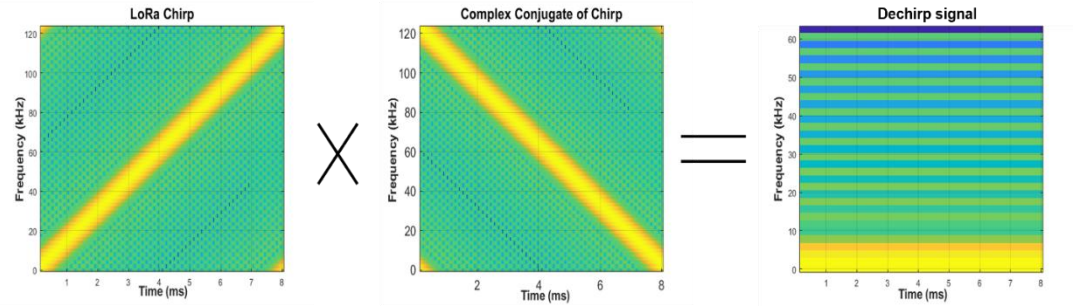

Figure 3.11: Illustration of Dechirped Operation.

(Figure 3.12) is showing an actual Message encoded on chirp signals using 10 symbols [600,400,500,555,1000,200,300,567,100,900] simulated using MATLAB.

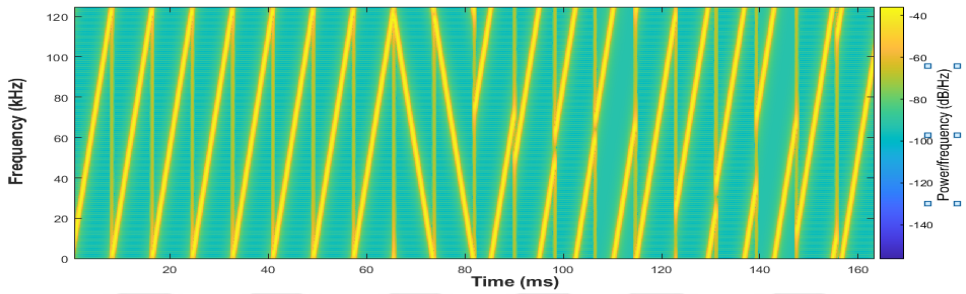

Figure 3.12: LoRa Message Encoded with 10 Symbols.

(Figure 3.13) is showing an actual standard LoRa Message decoding and DFT for the 10 symbols [600,400,500,555,1000,200,300,567,100,900] simulated using MATLAB.

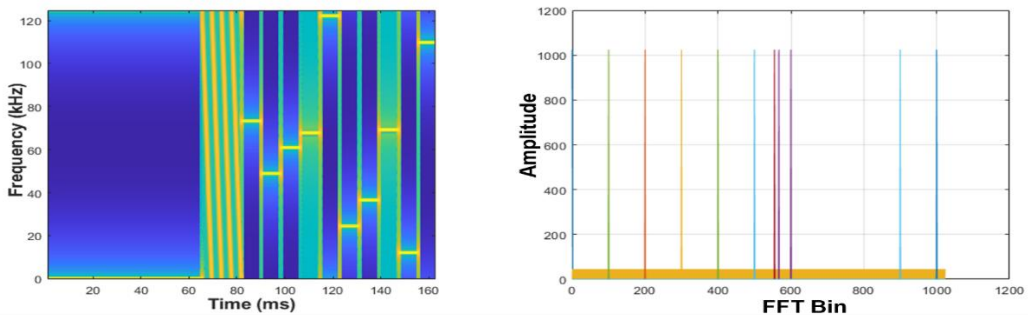

Figure 3.13: LoRa Message Decoded with 10 Symbols.

3.2.2 ICS-LoRa Modulation and Demodulation

The primary goal of ICS-LoRa was to provide extra chirp signals to allow a rise in the number of bits carried per symbol, therefore increasing the capacity for each ED[48]. Interleaved chirp spreading LoRa divides each LoRa chirp $\omega_q(n), q \in \{0,1, \dots 2^{SF} - 1\}$,

which has 2^{SF} samples, into four sub-chirps, each containing $\Delta = 2^{SF-2}$ samples. The equation for LoRa interleaved chirps $\phi_q(n)$ is provided in [48] as follows in Eq. (**3.20**).

$$\phi_q(n) = \begin{cases} \omega_q(n) & 0 \le n < \Delta \\ \omega_{(q+\Delta) mod 2^{SF}}(n) & \Delta \le n < 2\Delta \\ \omega_{(q+3\Delta) mod 2^{SF}}(n) & 2\Delta \le n < 3\Delta \\ \omega_q(n) & 3\Delta < n < 2^f \end{cases} \quad (3.20)$$

(Figure 3.14) illustrates an example of the standard LoRa chirp $\omega_q(n)$ and interleaved LoRa chirp $\phi_q(n)$ at spreading factor =7.

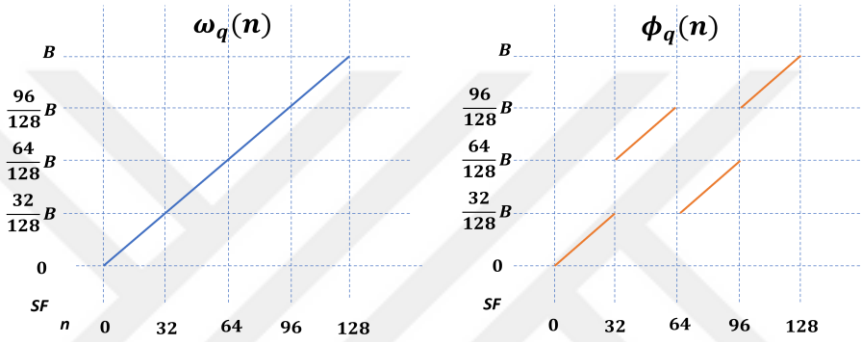

Figure 3.14: Illustrative Examples of $\omega_q(n)$ and $\phi_q(n)$ at SF=7.

At the receiver side, the de-interlevel operation accrues for the transmitted interleaved chirps spreading LoRa, which has the same equation for LoRa interleaved chirps $\phi_q(n)$ to reshape the interleaved chirps into standard LoRa chirps $\omega_q(n)$ followed by the Dechirping and DFT operation to decode the message signal. (Figure 3.15) Shows interleaved one LoRa chirp into ICS -LoRa at the transmitter side and de-interleaved ICS -LoRa at the receiver side, followed by deciphered operation simulated by MATLAB.

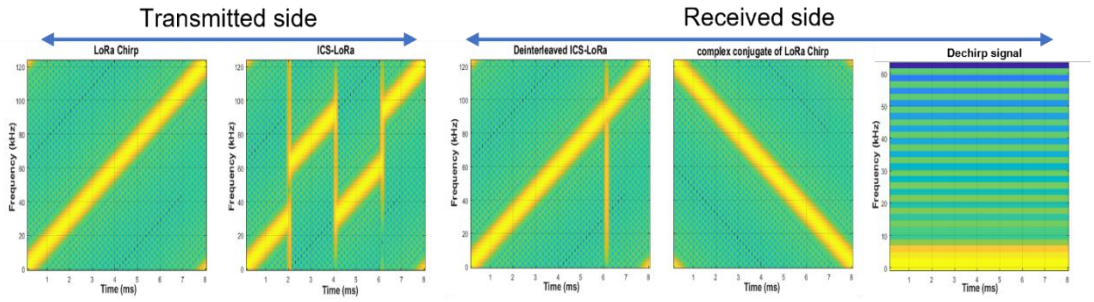

Figure 3.15: Illustration of Interleaved and Deinterleaved Followed by Dechirped Operation.

(Figure 3.16) is showing an actual Message encoded on interleaved chirp spreading LoRa signals using 10 symbols [600,400,500,555,1000,200,300,567,100,900] simulated using MATLAB.

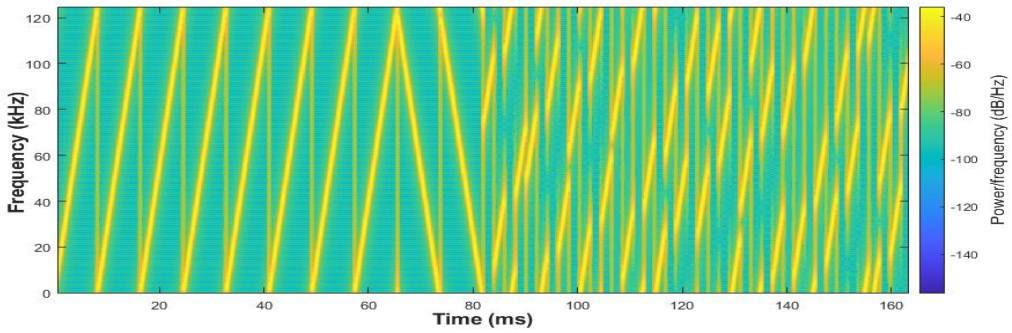

Figure 3.16: ICS-LoRa Message Encoded with 10 Symbols.

(Figure 3.17) is showing an actual ICS-LoRa Message decoding and DFT for the 10 symbols [600,400,500,555,1000,200,300,567,100,900] simulated using MATLAB.

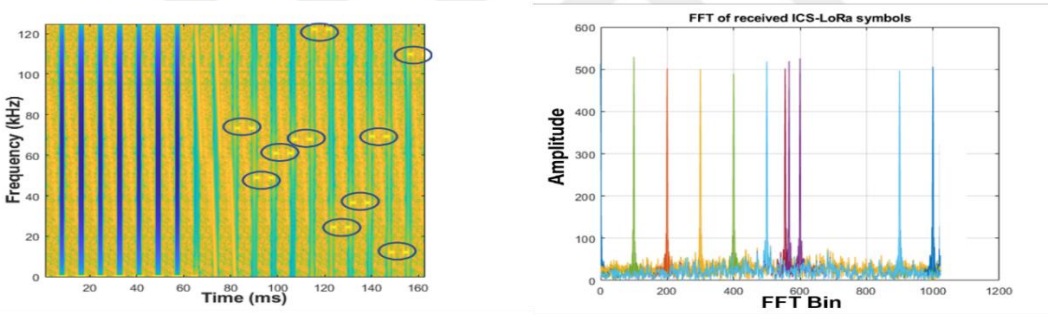

Figure 3.17: ICS-LoRa Message Decoded with 10 Symbols.

3.3 GRAY CODING

Coding is a symbolic way to represent discrete data. There are several types of codes. Gray code, sometimes known as Reflected binary code, is a numerical format in which each value varies from the preceding value by a single bit. Gray coding is inconvenient for mathematical calculations. It is a non-weighted code member belonging to the minimal change code family. Only one bit in the code group changes while moving from one step to another in this code[58]. Gray code has several beneficial uses, especially in wireless communication[59]. It is notable that in the situation of CSS modulation, the carriers and sampling frequency offset rather than white noise is what generates this mismatch between

neighboring symbols[60]. in LoRa, symbols could be represented as numbers from 0 to 2^{SF}, and by employing Gray coding to convert them to binary representation, we enhance the effectiveness of forwarding error correction methods and become able to correct a single incorrect bit in a codeword. The study of the method for converting binary to Gray is shown in the illustration in (Figure 3.18) below, which uses the binary number 11101 as an example and produces 10011 as the result. As an illustration, the Gray code operation for the binary number 11101 is shown in (Figure 3.18).

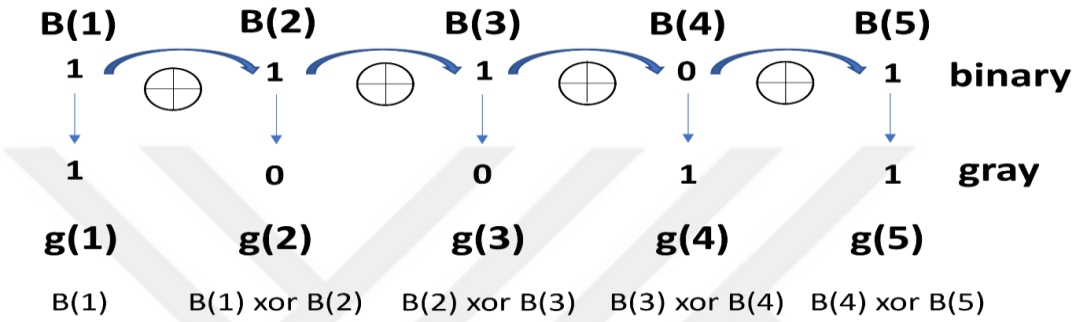

Figure 3.18: Gray Code Illustration.

In designing a binary-to-gray code converter, the number of inputs and outputs is based on the input and output values required. for example: two inputs (B_1, B_0) result in two gray outputs (G_1, G_0), whereas three inputs (B_2, B_1, B_0) result in three gray outputs (G_2, G_1, G_0). And there are four Gray-coded outputs for the four-bit binary inputs(B_3, B_2, B_1, B_0): (G_3, G_2, G_1, G_0). Tables 3.1 through 3.3 are a representation of the conversion of different bit inputs (2,3,4) to Gray code[61].

Table 3.1: Truth Table shows the Mapping Between two binary inputs and two Gray code outputs[61].

Binary inputs		**Gray outputs**	
$\mathbf{B_1}$	$\mathbf{B_0}$	$\mathbf{G_1}$	$\mathbf{G_0}$
0	0	0	0
0	1	0	1
1	0	1	1
1	1	1	0

Table 3.2: Truth table shows the mapping between three binary inputs and three Gray code outputs[61].

Binary inputs			Gray outputs		
B_2	B_1	B_0	G_2	G_1	G_0
0	0	0	0	0	0
0	0	1	0	0	1
0	1	0	0	1	1
0	1	1	0	1	0
1	0	0	1	1	0
1	0	1	1	1	1
1	1	0	1	0	1
1	1	1	1	0	0

Table 3.3: Truth table shows the mapping between four binary inputs and four Gray code outputs[61].

Binary inputs				Gray outputs			
B_3	B_2	B_1	B_0	G_3	G_2	G_1	G_0
0	0	0	0	0	0	0	0
0	0	0	1	0	0	0	1
0	0	1	0	0	0	1	1
0	0	1	1	0	0	1	0
0	1	0	0	0	1	1	0
0	1	0	1	0	1	1	1
0	1	1	0	0	1	0	1
0	1	1	1	0	1	0	0
1	0	0	0	1	1	0	0
1	0	0	1	1	1	0	1
1	0	1	0	1	1	1	1
1	0	1	1	1	1	1	0
1	1	0	0	1	0	1	0
1	1	0	1	1	0	1	1
1	1	1	0	1	0	0	1
1	1	1	1	1	0	0	0

3.4 PROPOSED MODEL

Our proposed system will combine coding with ICS-LoRa modulation in order to enhance system communication performance. Each part of our system is described below.

3.4.1 Transmitter Side

At the transmitter side of our system model, we proposed using binary reflected Gray code for the source data, as explained in (Figure 3.18) to enhance the data transmission with fewer errors before modulating data with LoRa Chirps. This data is encoded by LoRa chirp spread spectrum modulation, as shown in (Figure 3.12), followed by adding interleaver for these LoRa chirps to interleave the Chirps as explained in (Figure 3.14), and Eq. (3.20), which is a method proposed to make LoRa capacity increased and transmission without interference with the other six transmitted orthogonal spreading factors (7,8,9,10,11,12) after that the interleaved modulated chirps transmitted over the channels.

3.4.2 Channel

We examined the performance of our suggested system's data transmission over two different channels. AWGN channel and Rayleigh fading channel.

3.4.2.1 Additive White Gaussian Noise

Channel with Gaussian White Noise, or AWGN. This model simulates noises such as noisy environments and amplification noise exceptionally well, despite the complexity of noise. Additionally, the model may be supplemented with existing noise models, such as impulse noise or other widespread noise models[62].

3.4.2.2 Rayleigh Fading Channel

The Rayleigh fading model defines the type of fading that occurs when multipath is present. Multiple signal reflections and paths exist. The signal between the transmitter and receiver may classify as scattering. In such a scenario, there is no dominating signal path, requiring a statistical method to analyze the overall properties of the radio transmission medium[63]. We use The Jakes fading model in our simulation, a deterministic approach still extensively employed for modeling time-correlated Rayleigh fading waveforms. The model implies that

a Doppler effect occurs when Multiple rays of equal power arrive at a motion receiver with a random angle[64].

3.4.3 Receiver Side

On this side, the transmitted data encoded with Gray mapping, modulated with LoRa chirps, and interleaved by interleaver have been received. Initially, the data will be reconfigured using an interleaver to return it as conventional LoRa chirped instead of interleaved chirped, as illustrated in (Figure 3.15) Dechirping is performed by multiplying the transmitted LoRa signal by the complex conjugate of the signal's base chirp in order to decode the LoRa chirps, as shown in Eq. (3.15). (Figure 3.15) Then, a DFT operation is performed on the dechirped signal to detect the symbols, which are also detailed in Equation (3.18) and (Figure 3.17). Lastly, a Gray to binary converter is applied to the identified symbol to recover the original Binary source data. (Figure 3.19) shows our proposed system's block diagram with all stages.

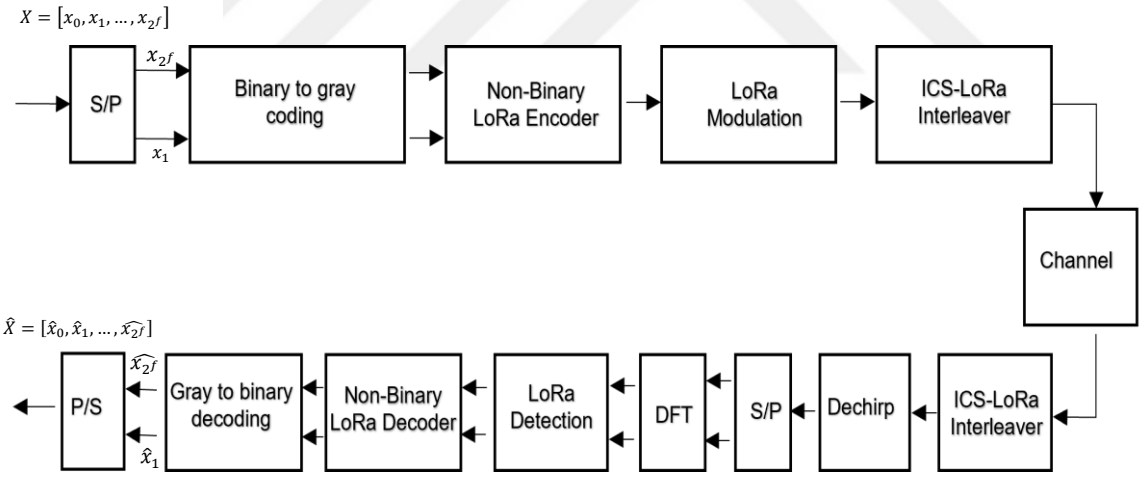

Figure 3.19: The Block Diagram of the Proposed System.

Finally, we compute the Bit Error Rate by using MATLAB for same data source with our proposed system in four conditions and make a full comparison between all conditions for all SNR points.

a. Computing BER for interleaved chirp spreading LoRa in AWGN channel without using Gray coding.

b. Computing BER for interleaved Chirp spreading LoRa in AWGN channel with using Gray coding.

c. Computing BER for interleaved Chirp spreading LoRa in Rayleigh fading Channel without using Gray coding.

d. Computing BER for interleaved Chirp spreading LoRa in Rayleigh fading Channel with using Gray coding.

4. SIMULATION AND RESULTS

MATLAB is utilized for our simulation. our study investigates the Bit Error Rate when using Gray coding for source data and encoding this data with interleaved chirp spreading LoRa. This simulation employs two separate channel types and six different spreading factors (7,8,9,10,11,12) for each channel.

4.1 AWGN CHANNEL

a. Spreading Factor =**7**

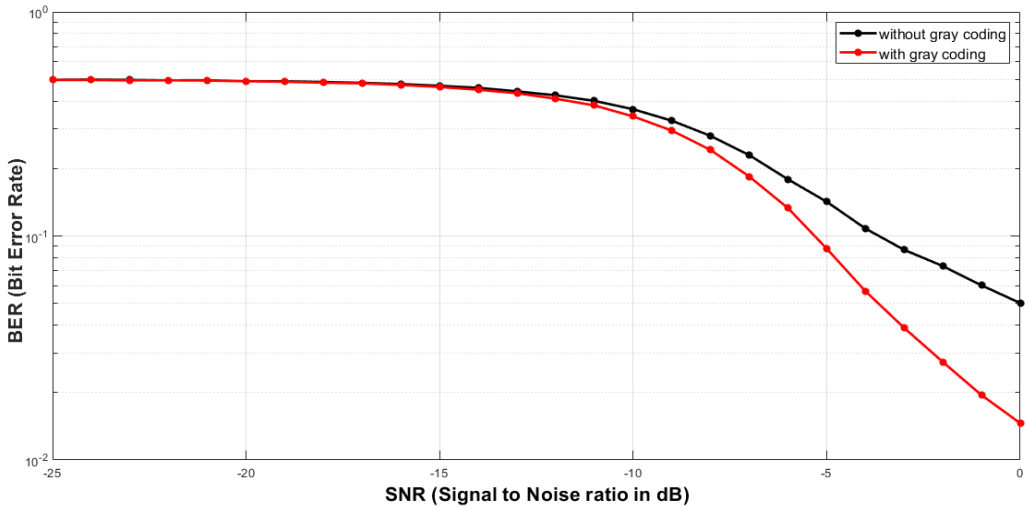

Figure 4.1: BER Vs SNR for AWGN channel and SF=7 with and without Gray coding.

(Figure 4.1) illustrates a comparison for interleaved chirp spreading LoRa communication Bit Error Rate at spreading factor 7 between the use of Gray coding for the transmitted source data and without it. The Black curve represents ICS-LoRa without the use of Gray coding, whereas the Red curve represents ICS-LoRa with the use of Gray coding.

Our results demonstrated that the use of Gray coding improves ICS-LoRa transmission by decreasing the BER, with the decrease starting at around -13 dB ,(Figure 4.2) represents the values of the BER reducing for all points of SNR, and it is clear that all points improve for all SNR Values, with this improvement increasing from -13 dB SNR with 0.0086 to a maximum of -5 dB SNR with 0.0543 and reducing gradually to SNR -1 dB with 0.0407.

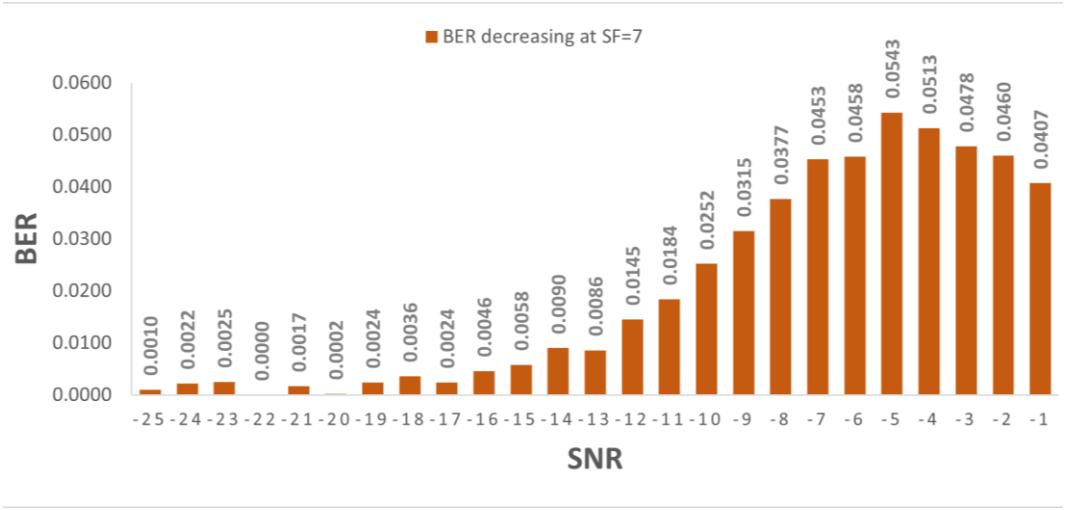

Figure 4.2: BER Enhancement using Gray coding in AWGN channel with SF=7.

b. Spreading Factor =**8**

c.

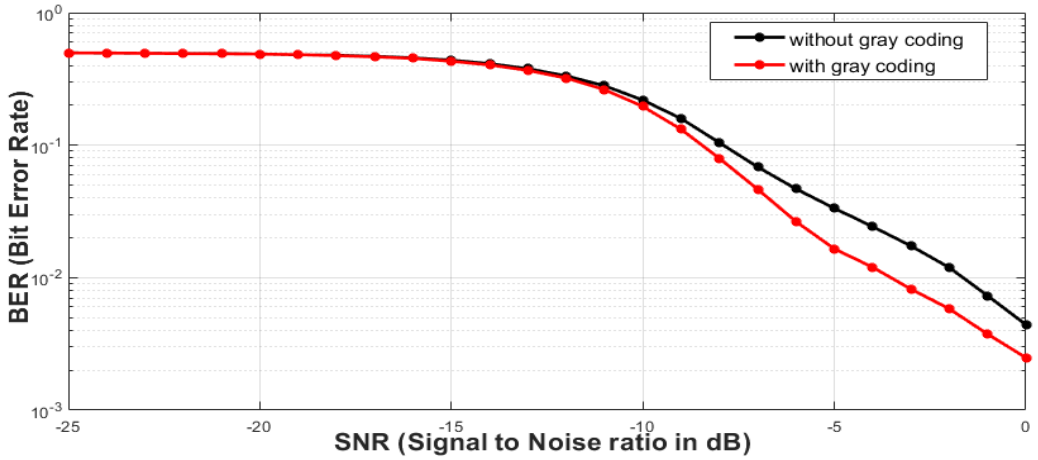

Figure 4.3: BER Vs SNR for AWGN channel and SF=8 with and without Gray coding.

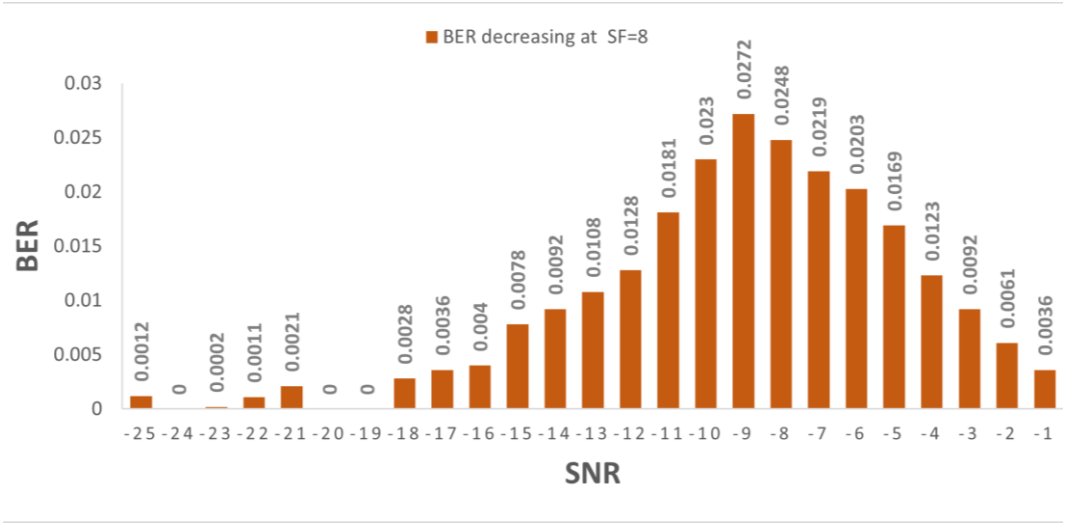

Figure 4.4: BER Enhancement using Gray coding in AWGN channel with SF=8.

(Figure 4.3) compare the BER for ICS-LoRa transmissions with Gray coding and without it when the spreading factor is 8. (Figure 4.4) demonstrates the improvement for each SNR value, with the BER improvement reaching its greatest at SNR=-9 dB, equivalent to 0.0272, and then steadily decreasing to 0.0036 at SNR= -1 dB

d. Spreading Factor =**9**

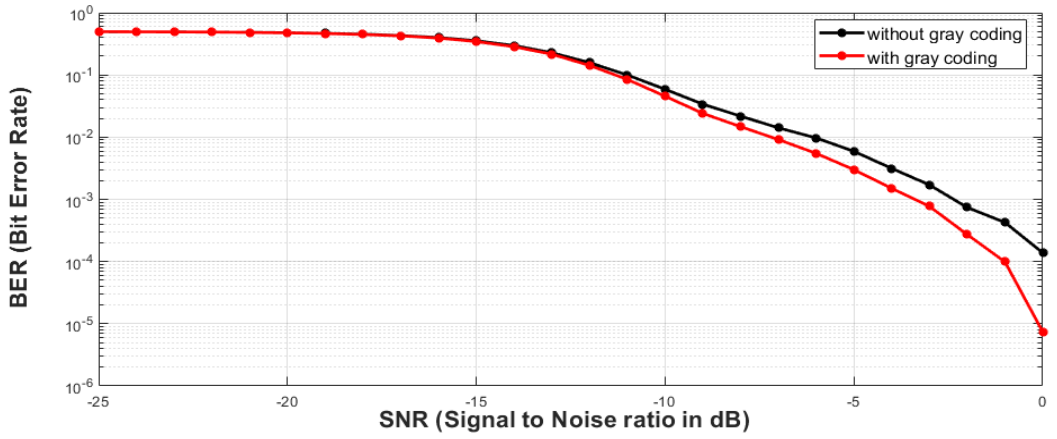

Figure 4.5: BER Vs SNR for AWGN Channel and SF=9 with and without Gray coding.

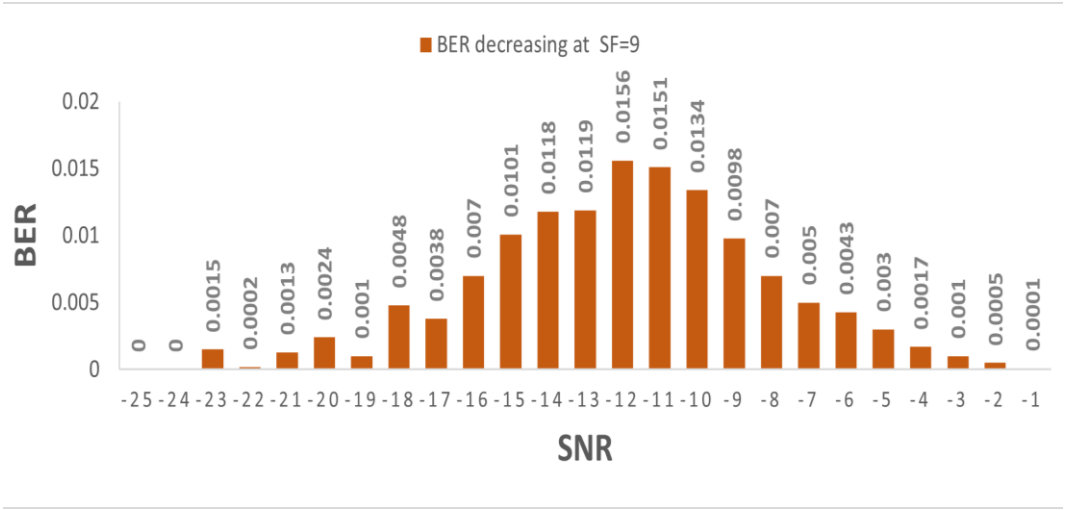

Figure 4.6: BER Enhancement using Gray coding in AWGN channel with SF=9.

When the spreading factor is 9, (Figure 4.5) compare the BER for ICS-LoRa transmissions with and without Gray coding. (Figure 4.6) demonstrates that the BER improved from (-24 to -17) dB, climbed to its maximum at SNR = -12 dB with 0.0156, and then reduced gradually to around 0 at SNR = -1 dB

e. Spreading Factor =**10**

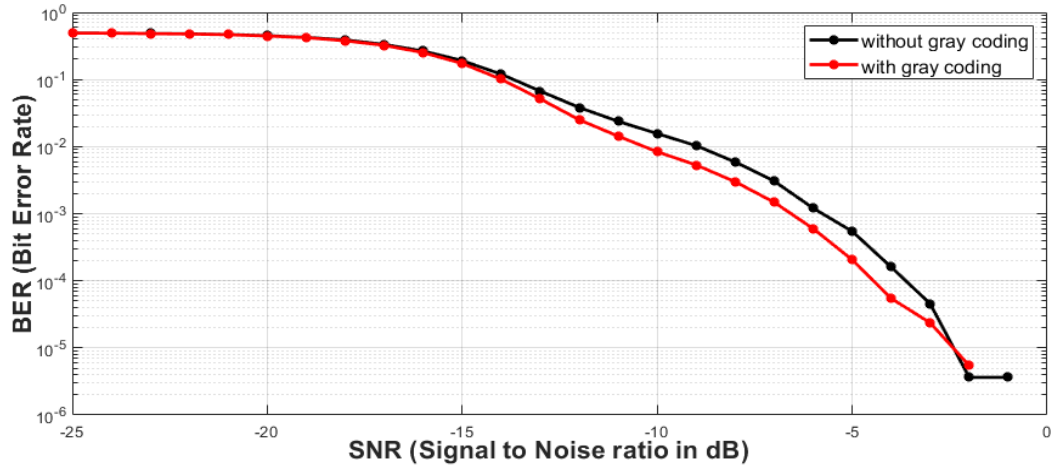

Figure 4.7: BER Vs SNR for AWGN channel and SF=10 with and without Gray coding.

(Figure 4.7) Comparing the BER for Gray-coded and uncoded ICS-LoRa transmissions at a spreading factor of 10. (Figure 4.8) illustrates a minor improvement from SNR (-25 to -19)

dB, followed by a significant increase to approximately 0.02, reducing BER at -14 dB SNR. Then the gain decreases gradually to around 0 at -5 dB SNR.

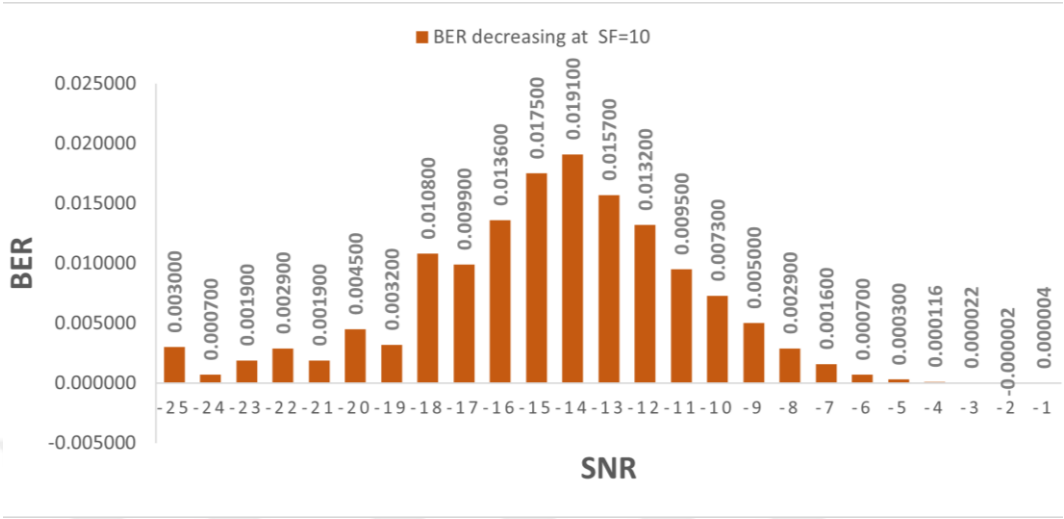

Figure 4.8: BER Enhancement using Gray coding in AWGN channel with SF=10.

f. Spreading Factor =**11**

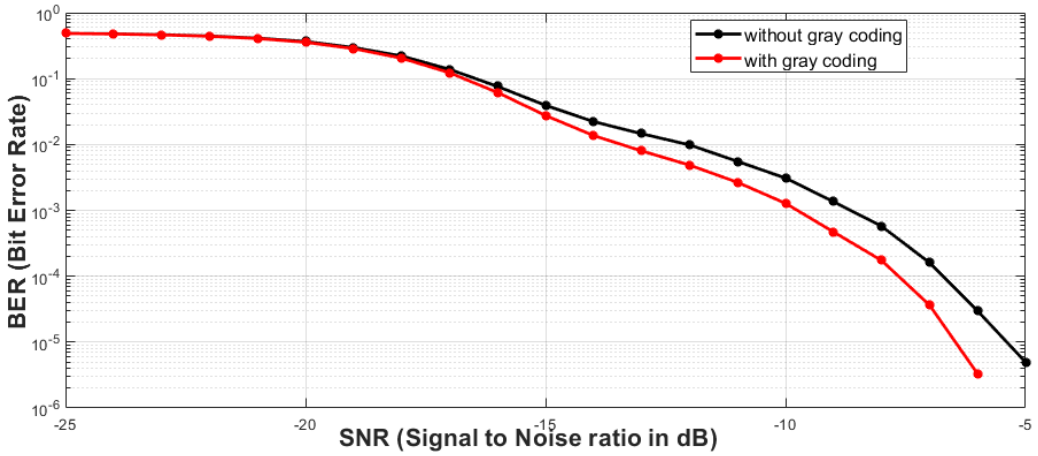

Figure 4.9: BER Vs SNR for AWGN channel and SF=11 with and without Gray coding.

(Figure 4.9). presented the bit error rate (BER) of Gray-coded and uncoded ICS-LoRa communications when a spreading factor is 11. (Figure 4.10). Shown that Starting at SNR -25 dB, there is a progressive increase of reducing BER, which reaches a high of 0.016 at SNR -18 dB, This improvement decreases gradually from -18 to -8 SNR and approaches around 0 at SNR -6 dB

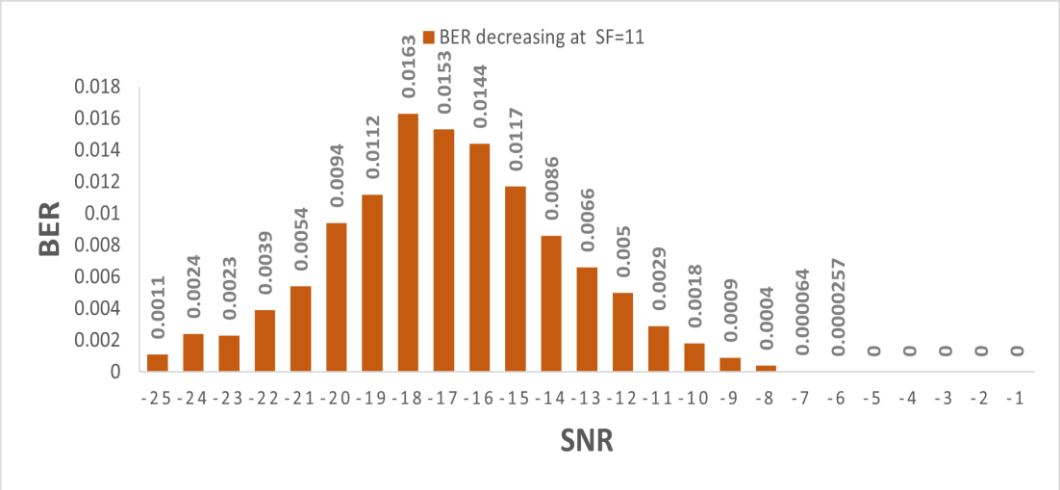

Figure 4.10: BER Enhancement using Gray coding in AWGN channel with SF=11.

g. Spreading factor =**12**

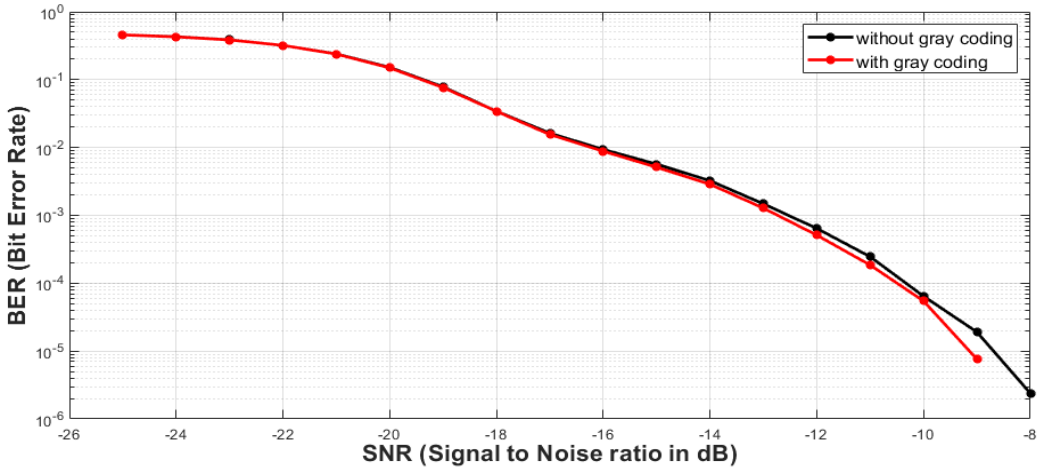

Figure 4.11: BER Vs SNR for AWGN channel and SF=12 with and without Gray coding.

(Figure 4.11). showed BER of Gray-coded and uncoded ICS-LoRa communications with a spreading factor equal to 12.as presented in (Figure 4.12). The BER decrease produces better results between SNR values (-21 to -19) around 0.002, whereas the enhancement decreases from SNR -18 to -11 and becomes 0 at SNR equal -9.

In (Figure 4.13). BER in ICS-LoRa with all spreading factors compared with and without the use of Gray coding in AWGN channel.

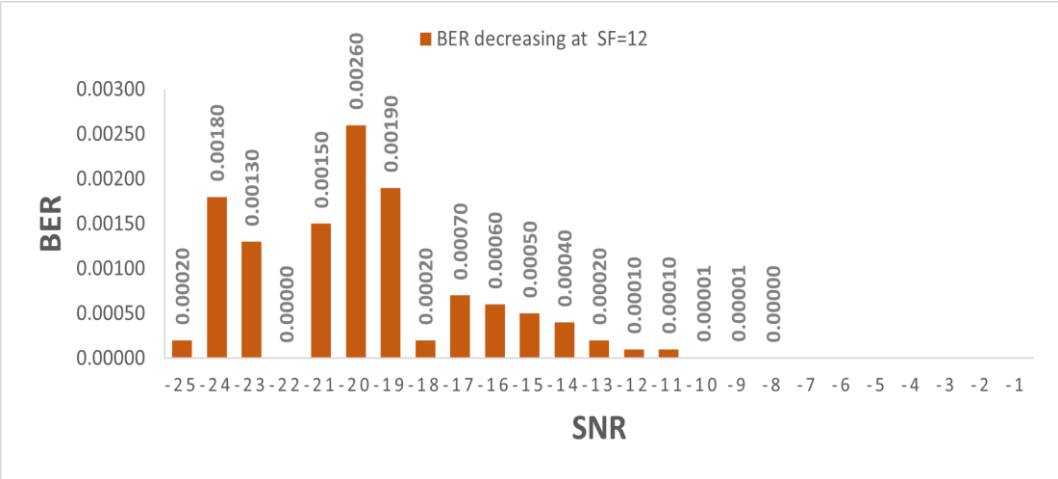

Figure 4.12: BER Enhancement using Gray coding in AWGN channel with SF=12.

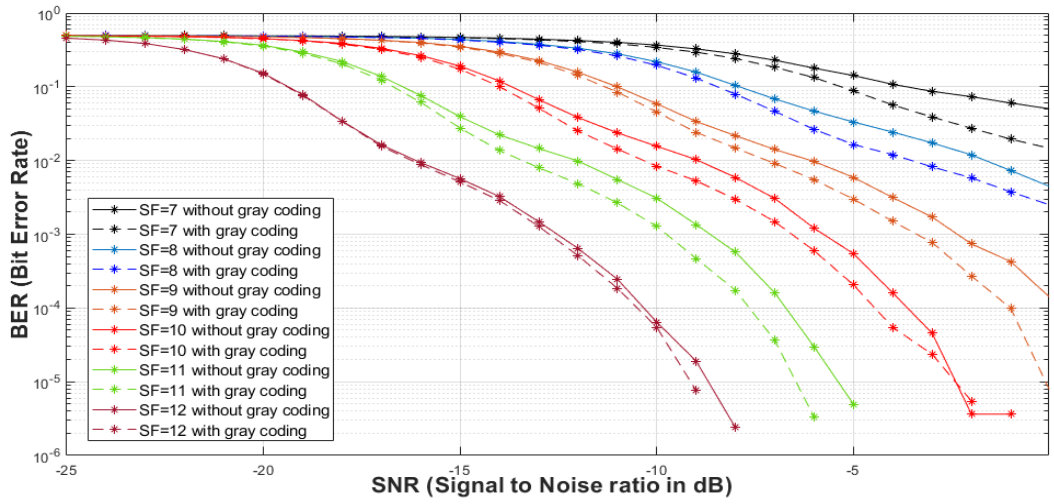

Figure 4.13: BER Enhancement for ICS-LoRa using Gray coding in AWGN channel with all Spreading Factors.

4.2 RAYLEIGH FADING CHANNEL

This section of our simulation will demonstrate the effects of adding Gray coding to source data on BER results for LoRa communication in Rayleigh fading channel using ICS-LoRa with all spreading factors (7,8,9,10,11.12).

a. Spreading Factor =**7**

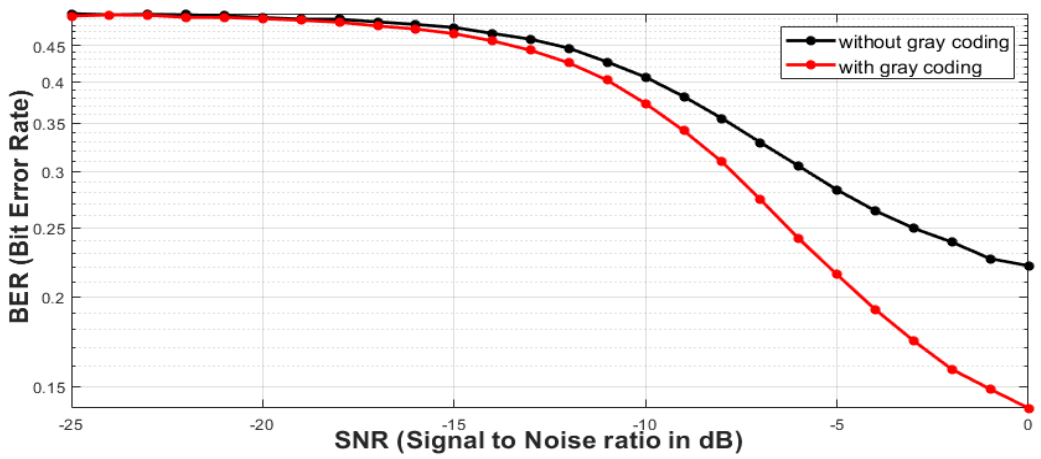

Figure 4.14: BER Vs SNR for Rayleigh channel and SF=7 with and without Gray coding.

(Figure 4.14). compared the BER performance of ICS-LoRa in the Rayleigh channel at a spreading factor of 7 with and without Gray coding. (Figure 4.15). There is a slight BER difference between utilizing Gray coding and not using it while the SNR is equal (-25 to -16) dB, and this enhancement increases steadily as the SNR increased, reaching its maximum at SNR -2 dB with a 0.0803 BER difference.

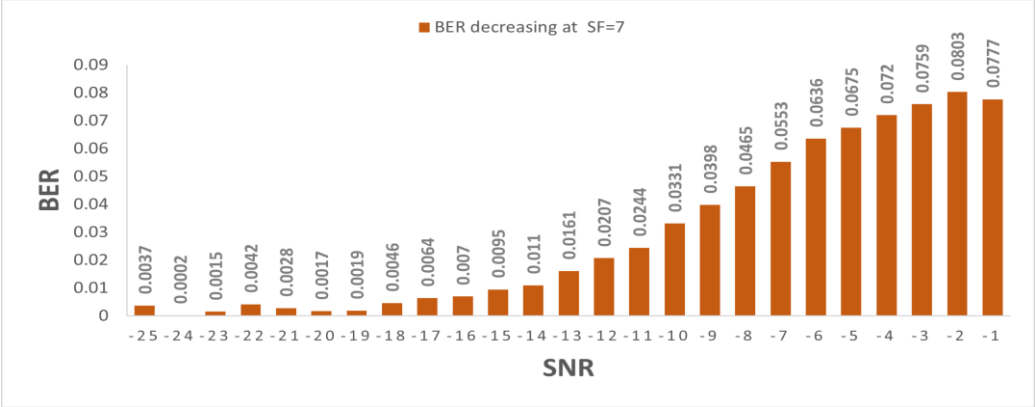

Figure 4.15: BER Enhancement using Gray coding in Rayleigh channel with SF=7.

b. Spreading Factor =**8**

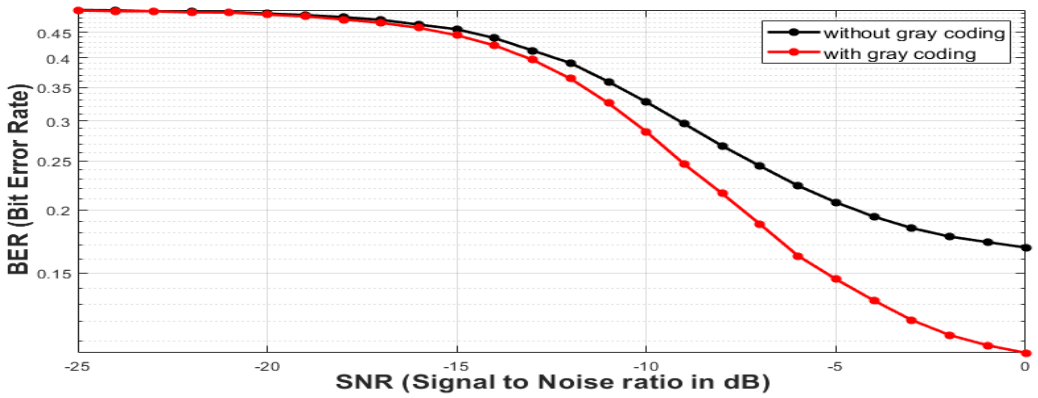

Figure 4.16: BER Vs SNR for Rayleigh channel and SF=8 with and without Gray coding.

In (Figure 4.16). ICS-LoRa modulation at SF=8 in the Rayleigh channel used to demonstrate the contrast between utilizing Gray coding and without it for LoRa communication. (Figure 4.17). Illustrated the BER reduction for each SNR point, showing a minor difference between SNR values (-25 to -15) dB, with an improvement that continued to grow from -14 dB as SNR values increased.

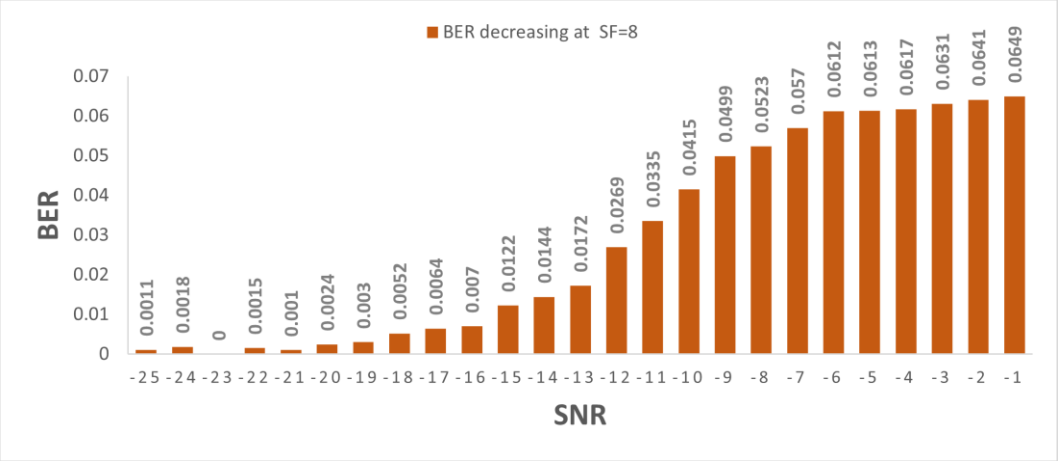

Figure 4.17: BER Enhancement using Gray coding in Rayleigh channel with SF=8.

c. Spreading Factor =**9**

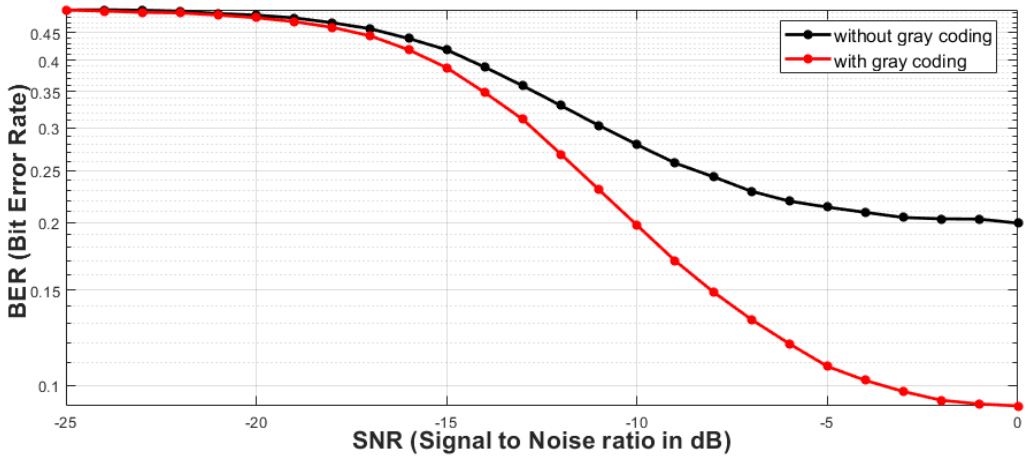

Figure 4.18: BER Vs SNR for Rayleigh channel and SF=9 with and without Gray coding.

(Figure 4.18). show the results of combining Gray coding with ICS-LoRa modulation to improve BER performance. (Figure 4.19). Displayed the actual decrease values in BER for each SNR point following the use of Gray coding for ICS-LoRa modulation, which demonstrated a slight improvement from SNR equal (-25 to -18) dB followed by an increase in improvement for all SNR points reaching 0.11 at SNR=-1 Db

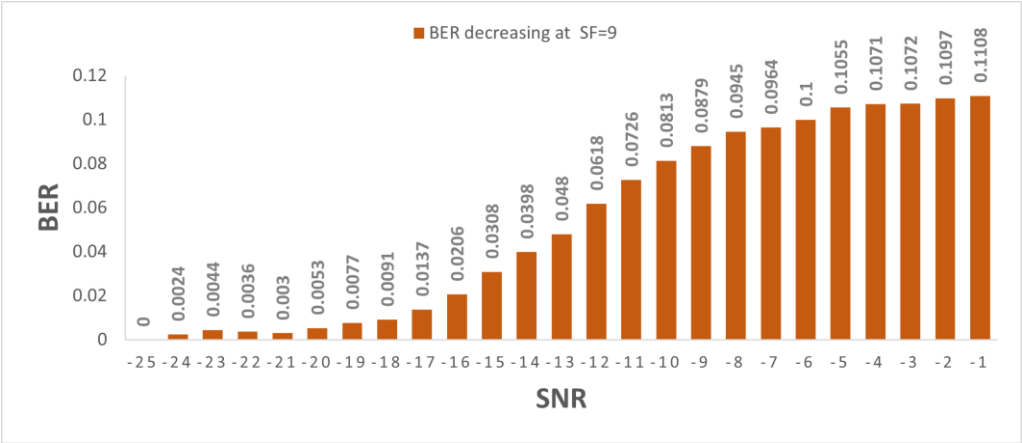

Figure 4.19: BER Enhancement using Gray coding in Rayleigh channel with SF=9.

d. Spreading Factor =**10**

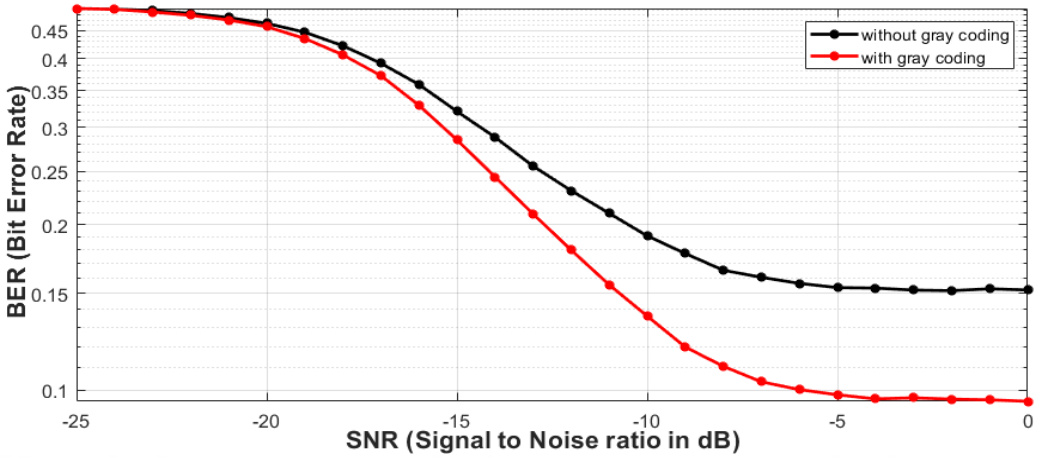

Figure 4.20: BER Vs SNR for Rayleigh channel and SF=10 with and without Gray coding.

In (Figure 4.20). the bit error rate (BER) for ICS-LoRa modulation with a spreading factor of 10 is illustrated with and without the application of Gray coding. (Figure 4.21). At a spreading factor of 10, the improvement begins to increase at an SNR of -25 dB, reaches a maximum difference of 0.0547 dB at an SNR of -9 dB, and then remains almost constant with the same values until the end of the SNR points.

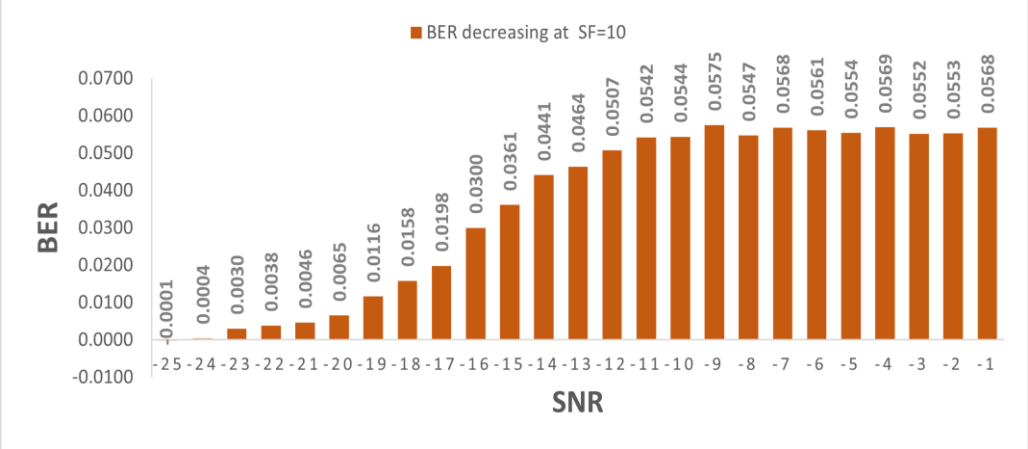

Figure 4.21: BER Enhancement using Gray coding in Rayleigh channel with SF=10.

e. Spreading Factor =**11**

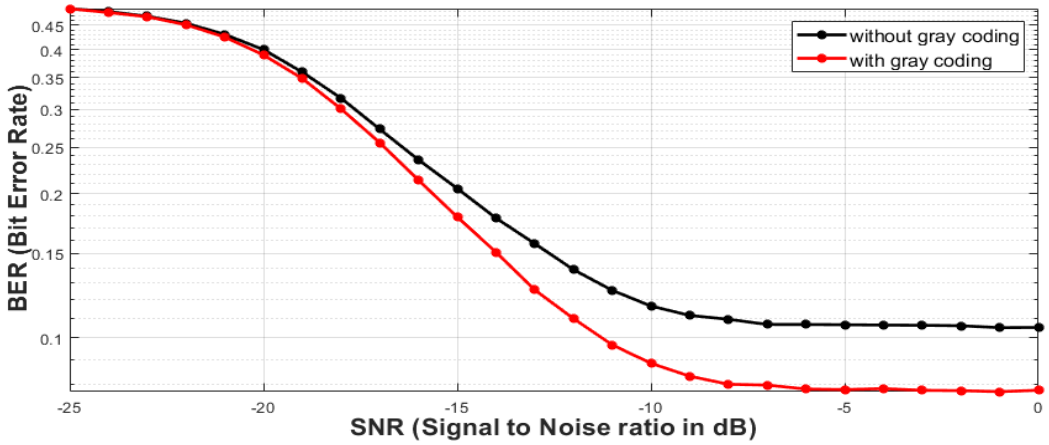

Figure 4.22: BER Vs SNR for Rayleigh channel and SF=11 with and without Gray coding.

(Figure 4.22). exemplify how Gray coding improves BER for ICS-LoRa modulation with a spreading factor of 11in Rayleigh channel. (Figure 4.23.) displays the precise deference values for the Rayleigh channel's BER at Sf=11, both with and without Gray coding. It demonstrates that improvement starts at SNR -25 dB and progresses steadily to the peak 0.0314 deference at SNR equal -13 dB. After that, improvement is nearly constant until SNR equals 0 dB.

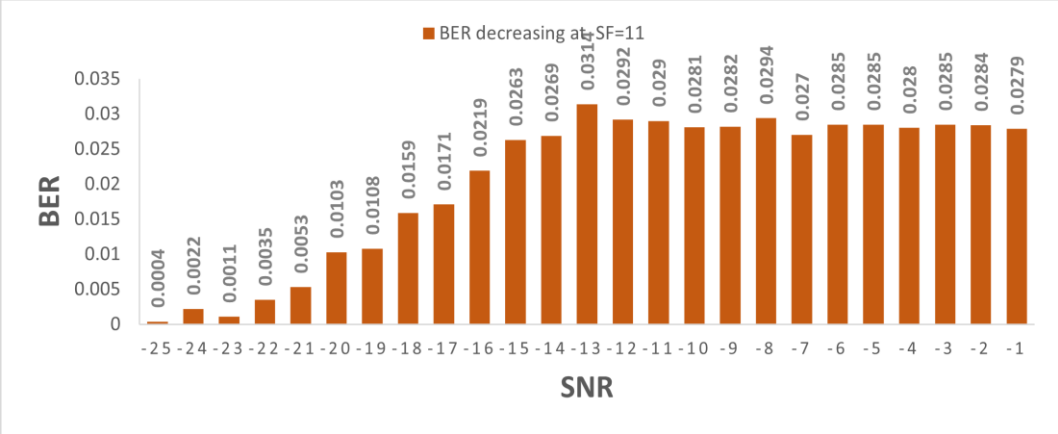

Figure 4.23: BER Enhancement using Gray coding in Rayleigh channel with SF=11.

f. Spreading Factor =**12**

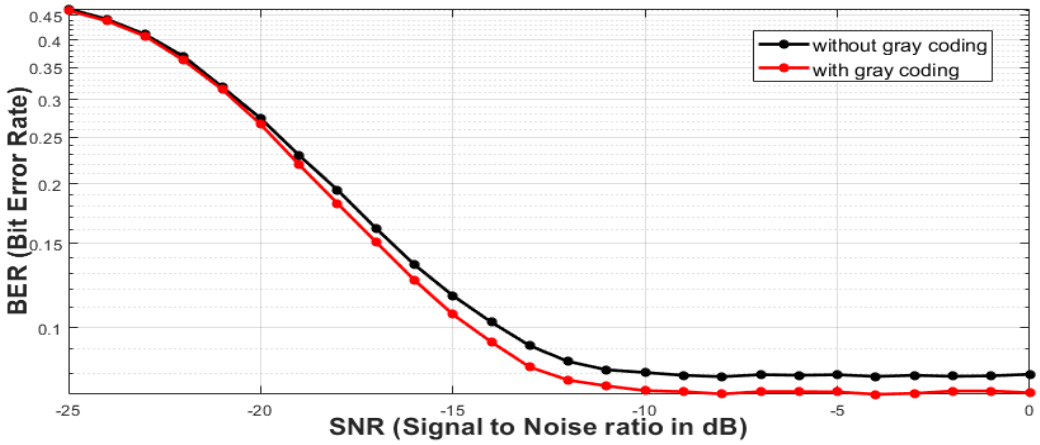

Figure 4.24: BER Vs SNR for Rayleigh channel and SF=12 with and without Gray coding.

(Figure 4.25). Displayed the actual differences in BER at SF=12 for ICS-Rayleigh LoRa's channel. This enhancement was nearly constant in SNR values (-25 to -21) dB around 0.003, then increased gradually to 0.0122 improvements at SNR equal -18 dB, then decreasing BER to 0.0061, at SNR equal -11 dB. The enhancement remains stable with the same difference of around 0.006 until the end of the curves.

In (Figure 4.26). BER in ICS-LoRa with all spreading factors compared with and without the use of Gray coding in Rayleigh fading channel.

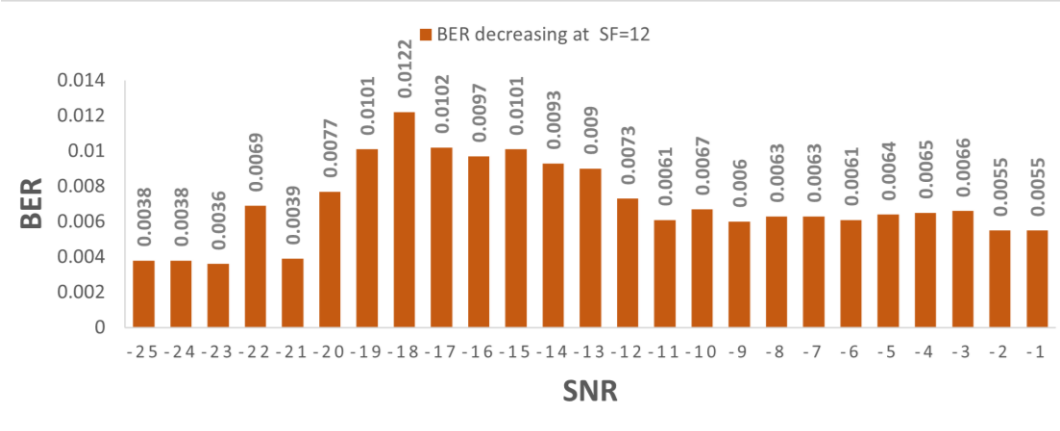

Figure 4.25: BER Enhancement using Gray coding in Rayleigh channel with SF=12.

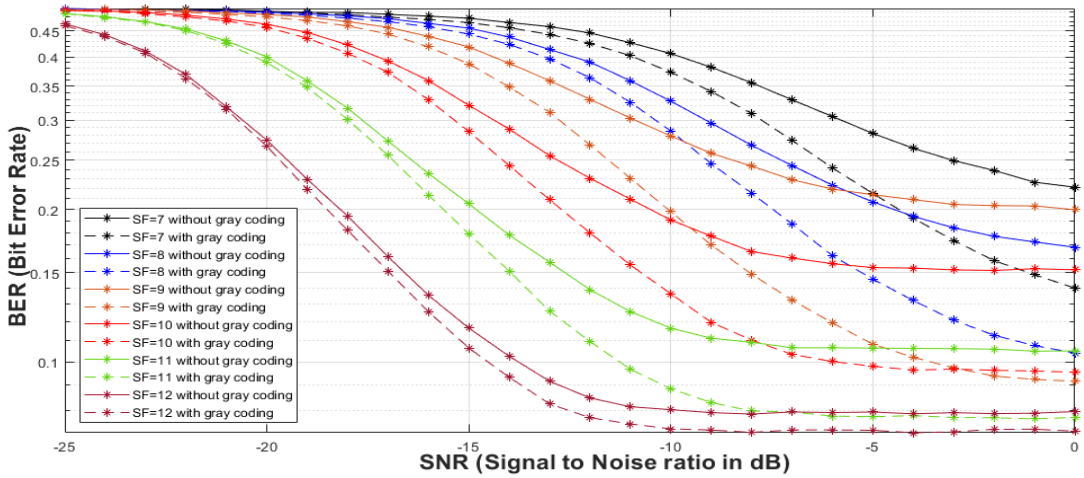

Figure 4.26: BER Enhancement for ICS-LoRa using Gray coding in Rayleigh channel with all Spreading Factors.

5. CONCLUSION

Interleaved chirp spreading LoRa (ICS-LoRa) has been presented as a method for increasing the capacity of LoRa-based low power wide area network (LPWAN). In this research, the bit error rate (BER) of ICS-LoRa is computed and reduced by using binary reflected Gray coding into the source information that is encoded in ICS-LoRa chirps. Ten symbols were encoded with Normal LoRa and ICS-Lora chirps and transmitted to test our system; on the receiving end, the same data were detected correctly for both ICS-Lora and Normal LoRa. To comprehend the properties of our suggested system clearly and accurately, This study employed two types of channels, AWGN and Rayleigh fading channel, and performed simulations for all LoRa spreading (7 to 12). the results of this study demonstrated that employing Gray coding for ICS-LoRa data transmission improves communication performance by reducing the Bit Error Rate. Our simulated findings show that the BER reduces with varying SF in different channel types; for instance, a 5.6% improvement in SF is 7, and a 3.5% improvement in SF is 11 for the AWGN channel. In addition, the results indicate that Gray coding with ICS-LoRa works better with interference and multipath channel, with a 7.1% improvement in SF equal 7 and a 15% improvement in SF equal 9 compared to a network that employs standard LoRa. In the future, we will attempt to implement our proposed system utilizing Software Defined Radio (SDR). and Try to use alternative types of coding, such as convolutional codes, hard- and soft-decision Viterbi algorithms, and turbo codes with ICS-LoRa, and compare them under different channel conditions then investigate how this coding affects all system properties performances, such as BER.

REFERENCES

[1] A. Mushtaq, S. H. Gupta, and A. Rajawat, “Design and Performance Analysis of LoRa LPWAN Antenna for IoT Applications,” in *2020 7th International Conference on Signal Processing and Integrated Networks (SPIN)*, Feb. 2020, pp. 1153–1156. doi: 10.1109/SPIN48934.2020.9071362.

[2] K. Mekki, E. Bajic, F. Chaxel, and F. Meyer, “A comparative study of LPWAN technologies for large-scale IoT deployment,” *ICT Express*, vol. 5, no. 1, pp. 1–7, 2019, doi: 10.1016/j.icte.2017.12.005.

[3] “Wireless Technology in IoT-LPWAN Solutions.” https://www.bridgethings.com/wireless-technology-in-iot-lpwan-solutions/

[4] R. S. Sinha, Y. Wei, and S. H. Hwang, “A survey on LPWA technology: LoRa and NB-IoT,” *ICT Express*, vol. 3, no. 1, pp. 14–21, 2017, doi: 10.1016/j.icte.2017.03.004.

[5] U. Raza, P. Kulkarni, and M. Sooriyabandara, “Low Power Wide Area Networks: An Overview,” *IEEE Communications Surveys and Tutorials*, vol. 19, no. 2, pp. 855–873, 2017, doi: 10.1109/COMST.2017.2652320.

[6] C. Pham, F. Ferrero, M. Diop, L. Lizzi, O. Dieng, and O. Thiare, “Low-cost antenna technology for LPWAN IoT in rural applications,” *Proceedings - 2017 7th International Workshop on Advances in Sensors and Interfaces, IWASI 2017*, pp. 121–126, 2017, doi: 10.1109/IWASI.2017.7974231.

[7] R. C. Juacaba Neto, P. Merindol, A. Gallais, and F. Theoleyre, “Scalability of LPWAN for Smart City Applications,” in *2021 International Wireless Communications and Mobile Computing (IWCMC)*, Jun. 2021, pp. 74–79. doi: 10.1109/IWCMC51323.2021.9498698.

[8] R. Sanchez-Iborra and M. D. Cano, “State of the art in LP-WAN solutions for industrial IoT services,” *Sensors (Switzerland)*, vol. 16, no. 5, 2016, doi: 10.3390/s16050708.

[9] LoRa Alliance Technical Commitee, “LoRaWAN 1.1 Specification,” *Technical document*, pp. 1–101, 2017, [Online]. Available: https://lora-alliance.org/wp-content/uploads/2020/11/lorawantm_specification_-v1.1.pdf

[10] “A technical overview of LoRa® and LoRaWAN™,” *LoRa Alliance*, 2015. https://lora-alliance.org/resource_hub/what-is-lorawan/

[11] “A DIGITAL REVOLUTION FOR OIL & GAS FROM SCADA TO INDUSTRIAL IOT,” 2021. https://lora-alliance.org/resource_hub/38843-2/

[12] L. A. Brief, “Wireless Gas Level Monitoring.” https://www.semtech.com/uploads/technology/LoRa/app-briefs/Semtech_Meter_GasLevel_AppBrief-FINAL.pdf

[13] R. P. Bennett, “Fire detection,” *Fire Detection*, 2011. https://www.semtech.com/uploads/technology/LoRa/app-briefs/Semtech_HB_FireDetection_AppBrief-FINAL.pdf

[14] S. Metering, “Water Flow Monitoring.” https://lora-developers.semtech.com/uploads/documents/files/Semtech_Meter_WaterFlow_AppBrierf-FINAL.pdf

[15] D. K. Singh, R. Sobti, A. Jain, P. K. Malik, and D. Le, “LoRa based intelligent soil and weather condition monitoring with internet of things for precision agriculture in smart cities,” *IET Communications*, vol. 16, no. 5, pp. 604–618, Mar. 2022, doi: 10.1049/cmu2.12352.

[16] N. Shah and S. Sundar, “Smart Electric Meter Using LoRA Protocols and lot applications,” in *2018 Second International Conference on Electronics, Communication and Aerospace Technology (ICECA)*, Mar. 2018, pp. 1178–1180. doi: 10.1109/ICECA.2018.8474749.

[17] K. M. Lee, “Distributed Computing Agriculture Water Spraying System using LORA Communication,” in *2022 International Conference on Electrical, Computer and Energy Technologies (ICECET)*, Jul. 2022, pp. 1–5. doi: 10.1109/ICECET55527.2022.9872687.

[18] Md. R. Islam, A. Matin, Md. S. Siddiquee, F. Md. S. Hasnain, Md. H. Rahman, and T. Hasan, "A Novel Smart Gas Stove with Gas Leakage Detection and Multistage Prevention System Using IoT LoRa Technology," in *2020 IEEE Electric Power and Energy Conference (EPEC)*, Nov. 2020, pp. 1–5. doi: 10.1109/EPEC48502.2020.9320109.

[19] N. Misran, M. S. Islam, G. K. Beng, N. Amin, and M. T. Islam, "IoT Based Health Monitoring System with LoRa Communication Technology," in *2019 International Conference on Electrical Engineering and Informatics (ICEEI)*, Jul. 2019, pp. 514–517. doi: 10.1109/ICEEI47359.2019.8988869.

[20] G. Callebaut and L. Van Der Perre, "Characterization of LoRa Point-to-Point Path Loss: Measurement Campaigns and Modeling Considering Censored Data," *IEEE Internet Things J*, vol. 7, no. 3, pp. 1910–1918, 2020, doi: 10.1109/JIOT.2019.2953804.

[21] M. Hassan, "LoRa and LoRaWAN," *Wireless and Mobile Networking*, no. December 2019, pp. 218–230, 2022, doi: 10.1201/9781003042600-16.

[22] T. Elshabrawy and J. Robert, "Enhancing LoRa Capacity using Non-Binary Single Parity Check Codes," *International Conference on Wireless and Mobile Computing, Networking and Communications*, vol. 2018-Octob, pp. 1–7, 2018, doi: 10.1109/WiMOB.2018.8589188.

[23] T. Elshabrawy and J. Robert, "Analysis of BER and Coverage Performance of LoRa Modulation under Same Spreading Factor Interference," *IEEE International Symposium on Personal, Indoor and Mobile Radio Communications, PIMRC*, vol. 2018-Septe, 2018, doi: 10.1109/PIMRC.2018.8581011.

[24] "Understanding ADR." https://lora-developers.semtech.com/documentation/tech-papers-and-guides/understanding-adr/

[25] F. Cuomo, M. Campo, A. Caponi, G. Bianchi, G. Rossini, and P. Pisani, "EXPLoRa: Extending the performance of LoRa by suitable spreading factor allocations," *International Conference on Wireless and Mobile Computing, Networking and Communications*, vol. 2017-Octob, 2017, doi: 10.1109/WiMOB.2017.8115779.

[26] D. Zorbas, G. Z. Papadopoulos, P. Maille, N. Montavont, and C. Douligeris, “Improving LoRa Network Capacity Using Multiple Spreading Factor Configurations,” *2018 25th International Conference on Telecommunications, ICT 2018*, pp. 516–520, 2018, doi: 10.1109/ICT.2018.8464901.

[27] T. Elshabrawy and J. Robert, “Capacity Planning of LoRa Networks with Joint Noise-Limited and Interference-Limited Coverage Considerations,” *IEEE Sens J*, vol. 19, no. 11, pp. 4340–4348, 2019, doi: 10.1109/JSEN.2019.2897156.

[28] G. Zhu, C. H. Liao, T. Sakdejayont, I. W. Lai, Y. Narusue, and H. Morikawa, “Improving the Capacity of a Mesh LoRa Network by Spreading-Factor-Based Network Clustering,” *IEEE Access*, vol. 7, pp. 21584–21596, 2019, doi: 10.1109/ACCESS.2019.2898239.

[29] R. Fernandes, R. Oliveira, M. Luís, and S. Sargento, “On the Real Capacity of LoRa Networks: The Impact of Non-Destructive Communications,” *IEEE Communications Letters*, vol. 23, no. 12, pp. 2437–2441, 2019, doi: 10.1109/LCOMM.2019.2941476.

[30] T. Elshabrawy and J. Robert, “Analysis of BER and Coverage Performance of LoRa Modulation under Same Spreading Factor Interference,” *IEEE International Symposium on Personal, Indoor and Mobile Radio Communications, PIMRC*, vol. 2018-Septe, 2018, doi: 10.1109/PIMRC.2018.8581011.

[31] T. Elshabrawy and J. Robert, “Closed-Form Approximation of LoRa Modulation BER Performance,” *IEEE Communications Letters*, vol. 22, no. 9, pp. 1778–1781, 2018, doi: 10.1109/LCOMM.2018.2849718.

[32] M. J. Faber, K. M. Van Der Zwaag, W. G. V. Dos Santos, H. R. D. O. Rocha, M. E. V. Segatto, and J. A. L. Silva, “A Theoretical and Experimental Evaluation on the Performance of LoRa Technology,” *IEEE Sens J*, vol. 20, no. 16, pp. 9480–9489, 2020, doi: 10.1109/JSEN.2020.2987776.

[33] V. Savaux and G. Ferre, “Simple Asymptotic BER Expressions for LoRa System over Rice and Rayleigh Channels,” *Wireless Telecommunications Symposium*, vol. 2021-April, pp. 7–10, 2021, doi: 10.1109/WTS51064.2021.9433680.

[34] G. Baruffa, L. Rugini, V. Mecarelli, L. Germani, and F. Frescura, “Coded LoRa Performance in Wireless Channels,” *IEEE International Symposium on Personal, Indoor and Mobile Radio Communications, PIMRC*, vol. 2019-Septe, pp. 1–6, 2019, doi: 10.1109/PIMRC.2019.8904298.

[35] G. Baruffa, L. Rugini, L. Germani, and F. Frescura, “Error probability performance of chirp modulation in uncoded and coded LoRa systems,” *Digital Signal Processing: A Review Journal*, vol. 106, p. 102828, 2020, doi: 10.1016/j.dsp.2020.102828.

[36] C. Zhang, J. Yue, L. Jiao, J. Shi, and S. Wang, “A Novel Physical Layer Encryption Algorithm for LoRa,” *IEEE Communications Letters*, vol. 25, no. 8, pp. 2512–2516, 2021, doi: 10.1109/LCOMM.2021.3078669.

[37] M. Xhonneux *et al.*, “A Two-User Successive Interference Cancellation LoRa Receiver with Soft-Decoding,” in *2021 55th Asilomar Conference on Signals, Systems, and Computers*, Oct. 2021, pp. 948–953. doi: 10.1109/IEEECONF53345.2021.9723151.

[38] S. An, Z. Lu, H. Wang, and Q. Yu, “A Turbo Coded LoRa-Index Modulation Scheme for IoT Communication,” in *2021 IEEE 21st International Conference on Communication Technology (ICCT)*, Oct. 2021, pp. 736–740. doi: 10.1109/ICCT52962.2021.9657863.

[39] L. H. de Oliveira Alves, J. L. Rebelatto, R. D. Souza, and G. Brante, “Network-Coded Cooperative LoRa Network With D2D Communication,” *IEEE Internet Things J*, vol. 9, no. 7, pp. 4997–5008, Apr. 2022, doi: 10.1109/JIOT.2021.3107784.

[40] J. M. de S. Sant’Ana, A. Hoeller, R. D. Souza, S. Montejo-Sanchez, H. Alves, and M. de Noronha-Neto, “Hybrid Coded Replication in LoRa Networks,” *IEEE Trans Industr Inform*, vol. 16, no. 8, pp. 5577–5585, Aug. 2020, doi: 10.1109/TII.2020.2966120.

[41] O. Afisiadis, A. Burg, and A. Balatsoukas-Stimming, “Coded LoRa Frame Error Rate Analysis,” *IEEE International Conference on Communications*, vol. 2020-June, no. 1, pp. 3–8, 2020, doi: 10.1109/ICC40277.2020.9148806.

[42] U. Noreen, L. Clavier, and A. Bounceur, “LoRa-like CSS-based PHY layer, Capture Effect and Serial Interference Cancellation,” in *European Wireless 2018; 24th European Wireless Conference*, 2018, pp. 1–6.

[43] P. Pongpunpurt, W. Khawsuk, and N. Sutthisangiam, “Development of Huffman code for Lora technology,” *Proceedings - 2019 IEEE SmartWorld, Ubiquitous Intelligence and Computing, Advanced and Trusted Computing, Scalable Computing and Communications, Internet of People and Smart City Innovation, SmartWorld/UIC/ATC/SCALCOM/IOP/SCI 2019*, pp. 1882–1887, 2019, doi: 10.1109/SmartWorld-UIC-ATC-SCALCOM-IOP-SCI.2019.00331.

[44] T. H. To and A. Duda, “Simulation of LoRa in NS-3: Improving LoRa Performance with CSMA,” *IEEE International Conference on Communications*, vol. 2018-May, pp. 1–7, 2018, doi: 10.1109/ICC.2018.8422800.

[45] O. Afisiadis, M. Cotting, A. Burg, and A. Balatsoukas-Stimming, “On the Error Rate of the LoRa Modulation with Interference,” *IEEE Trans Wirel Commun*, vol. 19, no. 2, pp. 1292–1304, 2020, doi: 10.1109/TWC.2019.2952584.

[46] A. Marquet, N. Montavont, and G. Z. Papadopoulos, “Investigating theoretical performance and demodulation techniques for LoRa,” *20th IEEE International Symposium on A World of Wireless, Mobile and Multimedia Networks, WoWMoM 2019*, 2019, doi: 10.1109/WoWMoM.2019.8793014.

[47] P. Savazzi, E. Goldoni, A. Vizziello, L. Favalli, and P. Gamba, “A wiener-based rssi localization algorithm exploiting modulation diversity in lora networks,” *IEEE Sens J*, vol. 19, no. 24, pp. 12381–12388, 2019, doi: 10.1109/JSEN.2019.2936764.

[48] P. Edward, M. El-Aasser, M. Ashour, and T. Elshabrawy, “Interleaved Chirp Spreading LoRa as a Parallel Network to Enhance LoRa Capacity,” *IEEE Internet Things J*, vol. 8, no. 5, pp. 3864–3874, 2021, doi: 10.1109/JIOT.2020.3027100.

[49] Semtech, “LoRa Modulation Basics AN1200.22,” *App Note*, no. May, pp. 1–26, 2015, [Online]. Available: https://www.frugalprototype.com/wp-content/uploads/2016/08/an1200.22.pdf

[50] B. Reynders and S. Pollin, “Chirp spread spectrum as a modulation technique for long range communication,” in *2016 Symposium on Communications and Vehicular Technologies (SCVT)*, Nov. 2016, pp. 1–5. doi: 10.1109/SCVT.2016.7797659.

[51] M. Alenezi, K. K. Chai, Y. Chen, and S. Jimaa, “Ultra-dense LoRaWAN: Reviews and challenges,” *IET Communications*, vol. 14, no. 9, pp. 1361–1371, Jun. 2020, doi: 10.1049/iet-com.2018.6128.

[52] D. H. Kim, E. K. Lee, and J. Kim, “Experiencing LoRa network establishment on a smart energy campus testbed,” *Sustainability (Switzerland)*, vol. 11, no. 7, 2019, doi: 10.3390/su11071917.

[53] “Semtech: SX1276/77/78/79,” 2015. [Online]. Available: https://www.semtech.com/products/wireless-rf/lora-connect/sx1272#documentation

[54] Semtech Corporation, “SX1272/3/6/7/8 LoRa Modem Design Guide, AN1200.13,” no. July, p. 9, 2013, [Online]. Available: https://www.rs-online.com/

[55] Semtech Corporation, “Understanding the LoRa Adaptive Data Rate,” *Understanding the LoRa Adaptive Data Rate Technical Paper*, no. December, pp. 1–15, 2019, [Online]. Available: https://lora-developers.semtech.com/documentation/tech-papers-and-guides/understanding-adr

[56] T. Elshabrawy and J. Robert, “Interleaved chirp spreading LoRa-based modulation,” *IEEE Internet Things J*, vol. 6, no. 2, pp. 3855–3863, Apr. 2019, doi: 10.1109/JIOT.2019.2892294.

[57] L. Vangelista, “Frequency Shift Chirp Modulation: The LoRa Modulation,” *IEEE Signal Process Lett*, vol. 24, no. 12, pp. 1818–1821, 2017, doi: 10.1109/LSP.2017.2762960.

[58] R. W. Doran, *Report Series The Gray Code*, no. March. 2007.

[59] M. H. Weik, “gray code,” in *Computer Science and Communications Dictionary*, Boston, MA: Springer US, 2000, pp. 691–691. doi: 10.1007/1-4020-0613-6_8053.

[60] R. Ghanaatian, O. Afisiadis, M. Cotting, and A. Burg, “LORA DIGITAL RECEIVER ANALYSIS AND IMPLEMENTATION Reza Ghanaatian , Orion Afisiadis , Matthieu Cotting , and Andreas Burg polytechnique f ′,” *ICASSP 2019 - 2019 IEEE International Conference on Acoustics, Speech and Signal Processing (ICASSP)*, pp. 1498–1502, 2019, [Online]. Available: https://ieeexplore.ieee.org/document/8683504/

[61] S. ISLAM, M. A.-A. SHAFI, and A. N. BAHAR, “Implementation of Binary To Gray Code Converters in Quantum Dot Cellular Automata,” *Journal of Today’S Ideas - Tomorrow’S Technologies*, vol. 3, no. 2, pp. 145–160, 2015, doi: 10.15415/jotitt.2015.32010.

[62] T. M. Cover and J. A. Thomas, “Gaussian Channel,” in *Elements of Information Theory*, Wiley, 2005, pp. 261–299. doi: 10.1002/047174882X.ch9.

[63] “Rayleigh Fading.” https://www.electronics-notes.com/articles/antennas-propagation/propagation-overview/rayleigh-fading.php

[64] P. Dent, G. E. Bottomley, and T. Croft, “Jakes fading model revisited,” *Electron Lett*, vol. 29, no. 13, pp. 1162–1163, 1993, doi: 10.1049/el:19930777.